Politecnico di Torino

Corso di Laurea Magistrale
in Ingegneria Aerospaziale

Tesi di Laurea Magistrale

CFD Streamlined Bodies Simulation and Optimization for Natural Laminar Flow provided by STAR-CCM+ and HEEDS softwares

Relatore: Prof. Paolo Baldissera

Candidato: Durante Leonardo

Marzo 2019

Acknowledgments

Eccoci arrivati alla parte più letta della tesi. Dimeneticherò sicuramente qualcuno ma vi assicuro che il lavoro dietro le quinte di questo lungo, lunghissimo, immenso viaggio (ho reso l'idea della lunghezza?!) è stato grandioso ed i miei ringraziamenti vanno a tutti voi.
Innanzitutto dedico un grazie a mamma e papà che continuamente mi hanno spronato ad andare avanti a suon di: "Se ce l'ha fatta tuo padre"; oppure con: "Sai chi si è laureato?", ed altre frasi "motivanti". Scherzi a parte grazie per il sostegno di questi anni e...lo sapete è inutile che lo scriva. Visto che bel figlio che avete cresciuto? :)
Un grazie inoltre va ai due moschettieri Emanuele e Ludovica (ludo tu leggi Ludovica ed Emanuele) che...sinceramente non c'è un motivo principale per ringraziarli talmente tante sono le cose per cui dovrei farlo! P.S. siete i miei fratelli preferiti!
Un grazie anche a quei tre disgraziati di Nunzio, Andrea e Davide (rigorosamente in ordine alfabetico) compagni di mille champions e battaglie.

Abstract

The main topic of this thesis is the solution at engineering problem of minimum drag axisymmetric vehicles design.
Drag reduction is only possible through manipulation of the vehicle shape, in order to delay viscous layer separation point.
An affusolage body will be invested at zeros angle by a costant speed flow.
In the first chapters is proposed a study of the physics problem, with an analysis of minimum drag bodies at difference Reynolds numbers, the boundary layer's evolution across body's length and it separation.
Later is proposed CFD analysis whith Gamma-Reθ transiction model using STAR-CCM+ and a subsequent optimization of the body's shape thanks to HEEDS software.

Contents

List of Figures

List of Tables

Introduction

Team Policumbent

This thesis born according to Policumbent team's needs to reduce drag force for its human powered vehicles prototypes. Policumbent is a students Team from Politecnico of Torino, orientated to the design and the realization of human powered vehicles and to ride the created prototypes [2]. Since 2009 Policumbent team continually develop new models, from C.O.R.A. (Cycling Optimized Recumbent Aeroshape) (2009-2010), to the most recently Taurus (2017-today). Since 2015 they are trying to overcome human speed limits in the middle of Nevada desert at about 1400 meters above sea level in the annual World Human Powered Speed Challenge (WHPSC), reaching very good places against other Universitary Team and also to overcome italian speed record twice in 2016 (126.90 km/h) and 2018 (133.26 km/h). In the Run mode Cyclists have to drive 5 miles in order to reach their top speed and the 200 m long timing zone.

Year	Prototype	Speed (km/h)
2015	PulsaR	116.19
2016	PulsaR	126.90
2017	Taurus	122.32
2018	Taurus	133.26

Table 1: WHPSC results

Figure 1: Pulse (2011/2012)

Figure 2: S-Trike (2013/2014)

Figure 3: PulsaR (2014/2016)

Figure 4: Taurus (2017-Today)

Chapter 1

Sate Of Art

Drag reduction by laminarization of the boundary layer plays an important role in aerodynamic aircraft design. For example, the current sailplanes high performances can only be obtained by extensive laminar flow regions on suction and pressure sides of the wing. With the application of laminar airfoil sections the drag contribution of the fuselage will achieve a significant amount.[1]
Laminar to turbulent transition is a complex and yet not fully understood phenomenon.

1.1 World's Fastest Human-Powered Bike: Eta

Eta is the World's fastest human-powered bike with a maximum speed of 144 Km/h. The bike, named Eta for the Greek symbol used to denote efficiency in engineering, uses a highly aerodynamic shape and coating, an ergonomic reclining position for the rider, and modern composite materials such as carbon fiber weaves to provide as much power transfer as possible through the stiff bike frame.[3]
The most important part of making the vehicle faster than an ordinary bicycle is by eliminating flow separation over the body. Doing this can decrease the drag over a given size object by over an order of magnitude!
To design the pressure profiles of the vehicle to eliminate flow separation, the Stratford-Smith criterion was used. This criterion is an analytic formulation to determine when the flow is on the verge of separation based upon the pressure gradient along streamlines.

Once the separation pressure drag over the vehicle is eliminated, the shear surface drag becomes the largest drag component we see on the vehicle. This is the drag acting tangentially to the surface of the vehicle caused by the viscosity of the air moving across it. The shear drag on the vehicle is determined by the state of the boundary layer over the surface. The boundary layer grows to about a centimetre thick at the trailing edge of our vehicles and can accounts for the vast majority of our aerodynamic drag. The boundary-layer begins laminar at the nose but may eventually destabilize into a turbulent boundary layer which has many times more drag.

To design for laminar flow, a favourable pressure gradient (decreasing pressure) along surface streamlines is desirable to assist in the stability of the laminar boundary layer and prevent it from transitioning to turbulence. In the laminar region, the shape of the pressure profiles are modelled based upon two-dimensional airfoils are designed for extensive runs of laminar flow (most notably NACA 6-Series airfoils). These typically follow a constant favourable (negative) pressure gradient which allows for a similar amount laminar flow across various angles of attack.

Another thing to mention about extensive runs of laminar flow is its contribution to reducing flow separation. Greater amounts of laminar flow substantially reduces the momentum boundary-layer thickness (a measure of how much of the flow's momentum is trapped in the boundary-layer) and allows for a shorter tail and a more aggressive pressure recovery.

All put together, the pressure profiles Eta was designed for boast a linear laminar flow region combined with a Stratford pressure recovery. [4]

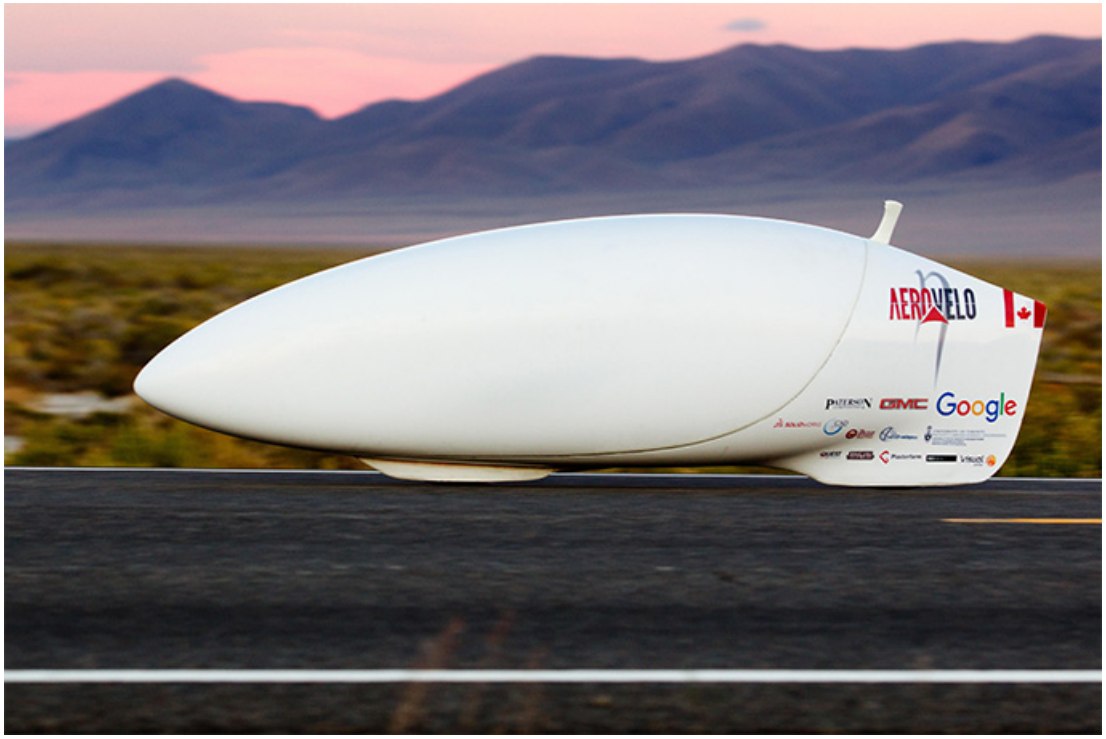

Figure 1.1: Eta

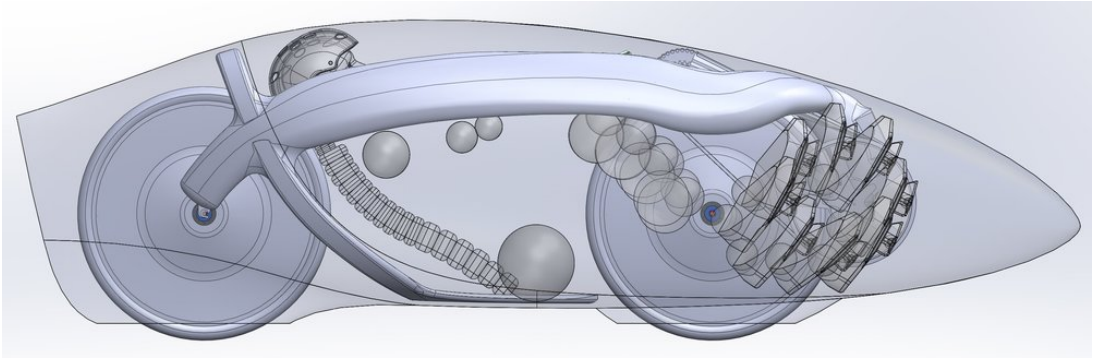

Figure 1.2: Eta Inside

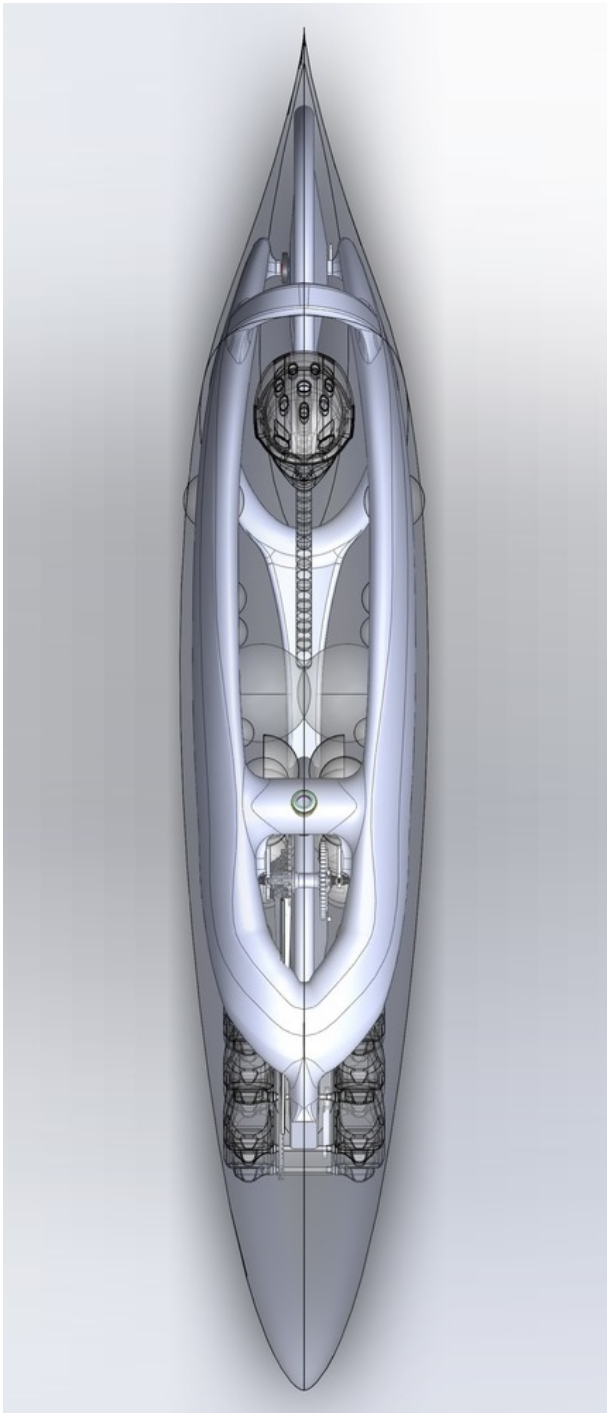

Figure 1.3: Eta top View

1.2 Drag Coefficient and Reynolds Number

Plotting drag coefficient of an azisymmetric body for Reynolds number's rage, we can notice three different regions.
For Reynolds number lower than $5 \cdot 10^6$ is possible to have extensive laminar flow thanks to a low skin friction.
Increasing Reynolds number, transiction points move towards the body nose increasing drag coefficient.

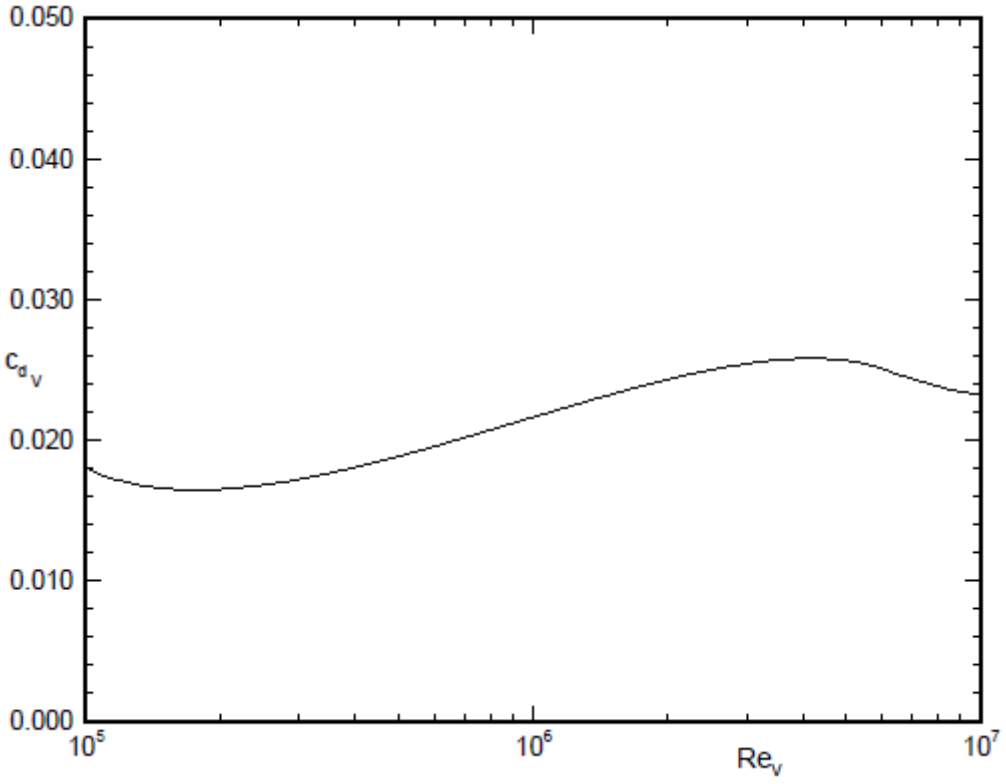

Figure 1.4: Drag Coefficient versus Reynolds Number

In Reynolds $> 10^7$ region bundary layer is almoust fully turbolent. An important task for aerodynamics is to determinate how to shape the body geomery to delay trasiction and to realize extensive laminar flow.
However, it is not known to what extent the theoretically evaluated laminar flow can be realised with actual airship applications with a certain degree of surface waviness. For the shape optimzations presented in this work, it became obvious

that one-point optimizations for a single Reynolds number lead to bodies which are inconvenient or even unusable outside of their design point.
This is especially true for laminar bodies at low Reynolds numbers.
Following is reportded shaping optimization at various Reynolds Numbers.[5]

- Regime I: $1 \cdot 10^6 < Re < 3.16 \cdot 10^6$
- Regime II: $3.16 \cdot 10^6 < Re < 1 \cdot 10^7$
- Regime III: $1 \cdot 10^7 < Re < 3.16 \cdot 10^7$
- Regime IV: $3.16 \cdot 10^7 < Re < 1 \cdot 10^8$

The initial source distribution chosen for design regime I corresponded to an ellipsoid-like starting geometry with a small length-to-diameter ratio of L/D=2.3.

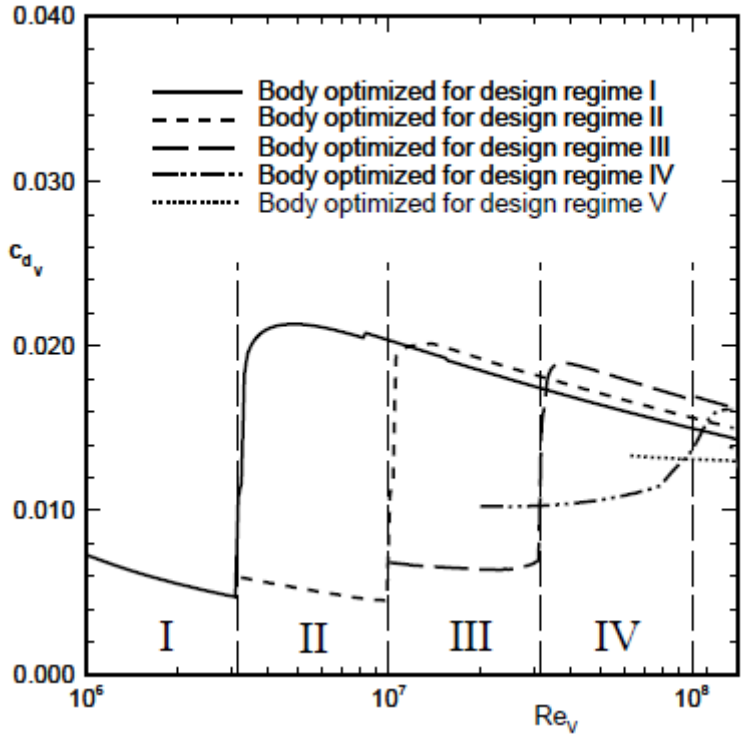

Figure 1.5: Shaping Optimization versus Reynolds Number

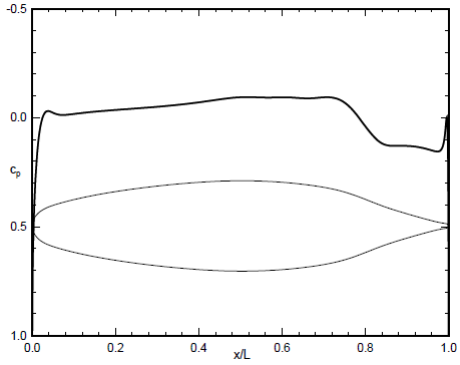

Figure 1.6: Optimizated Body Design Regime I

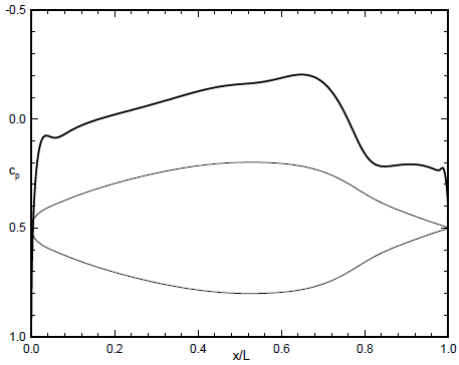

Figure 1.7: Optimizated Body Design Regime II

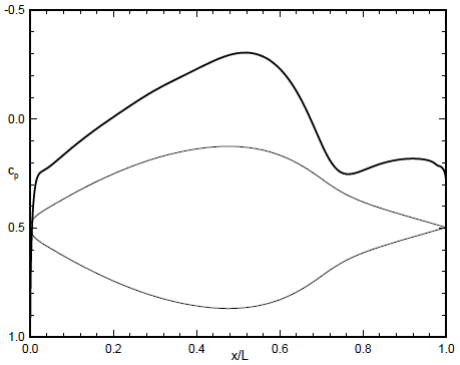

Figure 1.8: Optimizated Body Design Regime III

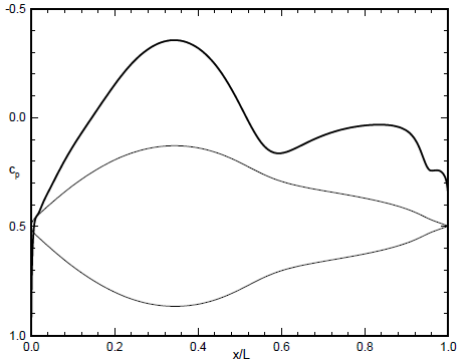

Figure 1.9: Optimizated Body Design Regime IV

When comparing body contour and pressure distribution, it can be noted that minimum pressure coefficient occurs downstream of the maximum thickness point. Increasing Reynolds number, in order to maintain laminar flow, the amount of favorable pressure gradient in the forebody region has to be enlarged. This can be realized in two different ways:

- increasing the body diameter
- moving the maximum thickness point upstream

Chapter 2

Physics problem

2.1 Aerodynamic Drag

Aerodynamic drag is the fluid drag force that acts on any moving solid body in the direction of the fluid freestream flow. From the body's perspective (near-field approach), the drag results from forces due to pressure distributions over the body surface. The surrounding fluid exerts pressure forces and viscous forces on an object. The components of the resultant force acting on the object are the drag force and the lift force and both are influenced by the size and shape of the object and the Reynolds number of the flow.

$$F_D = \frac{1}{2}\rho U^2 C_D A \tag{2.1}$$

$$R_e = \frac{\rho U D}{\nu} \tag{2.2}$$

Where:

- F_D: aerodynamic force
- ρ: fluid density
- U: body's speed
- c_D: aerodynamic coefficient

- A: cross sectional area
- Re : Reynolds Number
- ν : dynamic viscosity.

The drag force is due to the pressure and shear forces acting on the surface of the object.

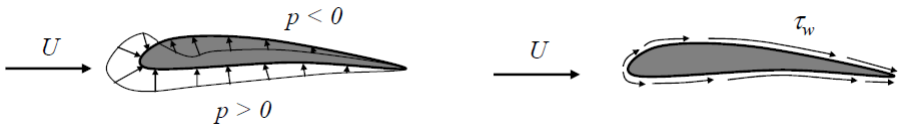

Figure 2.1: Pressure and shear forces acting on body surface

In order to predict corretly the drag, we need to known the pressure field and the surface shear stress on the object.

$$F_{D,viscous} = A \cdot \tau_w \tag{2.3}$$

$$F_{D,pressure} = \int_A p \cdot da_n \tag{2.4}$$

2.2 Laminar and Turbulent Flow

The primary characteristic of laminar flow is a streamlined flow, lacking any swirls or cross currents. If one imagines different layers of a fluid, divided into rows/cylinders at various radii, the layers of the fluid wouldn't mix. The fluid would flow without interference or disturbance, and the path of the flow wouldn't have any swirls or cross currents.
The layers or "tubes" of the fluid would still flow at different speeds, even though they wouldn't cross or intersect. The central, innermost layer would have the fastest flow speed while the outer layers would have a much slower flow speed (sometimes hardly moving at all). In general, the velocity of a fluid with laminar flow is extremely low.[11] In fluid dynamics, laminar flow occurs when a fluid flows in parallel

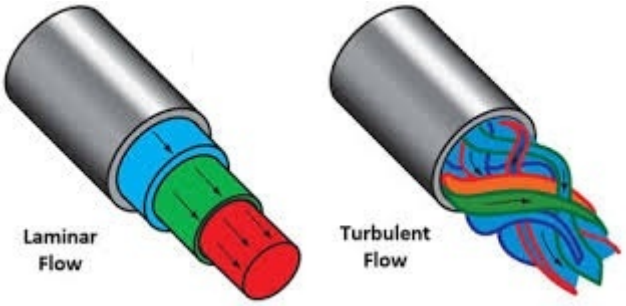

Figure 2.2: Laminar vs Turbulent Velocity Profile

layers, with no breaks between the layers. The fluid tends to flow without lateral mixing, and adjacent layers slide past one another like playing cards. There are no cross-currents perpendicular to the direction of flow, nor eddies or swirls of fluids. In laminar flow, the motion of the particles of the fluid is very orderly with particles close to a solid surface moving in straight lines parallel to that surface. Laminar flow is a flow regime characterized by high momentum diffusion and low momentum convection.
Laminar Flow could be described as the flow of a fluid whenever each and every particle belonging to the fluid is a follower of a consistent course, routes which usually under no circumstances obstruct with one another. One consequence of laminar movement would be that the speed belonging to the fluid is actually constant at any time inside fluid whereas on the other hand Turbulent Flow could be described as the uneven, unfrequented movement of fluid which is seen as a small whirlpool

areas. The speed of such a fluid is unquestionably not necessarily constant at each and every point. Turbulent flow is characterized by the chaotic and rough movement of particles through a region. Imagining layers of a fluid again, you can think of the various layers mixing with one another, with a heavy amount of friction existing between the boundaries of the different layers. Molecules are thrown around in an irregular fashion, and whirlpools and waves can easily be found within the flow. Fluids that are in turbulent flow have a substantial amount of kinetic energy within them. As long as this energy persists, the flow will continue to be turbulent and irregular. Once the energy is used up, the flow transitions to a laminar state. The velocity of a turbulent fluid is typically high, equalizing as it transitions to a laminar flow state.

When a fluid is flowing through a closed channel such as a pipe or between two flat plates, either of two types of flow may occur depending on the velocity and viscosity of the fluid: laminar flow or turbulent flow. Laminar flow tends to occur at lower velocities, below a threshold at which it becomes turbulent. Turbulent flow is a less orderly flow regime that is characterised by eddies or small packets of fluid particles, which result in lateral mixing. In non-scientific terms, laminar flow is smooth, while turbulent flow is rough.

Fluids frequently do transition between turbulent and laminar flows. This transition between the two different kinds of flows is impacted by a variety of different variables. Changes in the flow of a fluid may be driven by interactions with an object moving through the air, causing layers of a fluid to mix or straighten out as it moves along. For instance, while the air that moves over the wing of a plane is generally flowing in a laminar fashion, the air surrounding the plain is probably flowing turbulently. The tips of airplane wings often create a tip vortex, which causes the air in that region to begin flowing turbulently.

2.3 Boundary Layers and Separation

Now the body is invested by the flow. According to slip condition, the fluid velocity on surface body is zero; the layers closer to the wall start moving right away due to the no-slip boundary condition and later start moving the layers farther away from the wall. The distance from the wall that is affected by the motion is also called viscous diffusion length. The layers close to the wall are dragged along while the layers farther away from the wall move with a lower velocity. The viscous layer develops as a result of the no-slip boundary condition at the wall. [7]
When viscous layer velocity reaches the 99% of undisturbed speed the viscous layer ends.

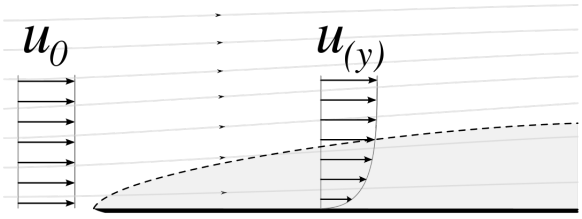

Figure 2.3: Velocity Profile

Exact equations for velocity profile in viscous boundary layer were derived by Stokes in 1881.

From the Navier-Stokes equation:

$$\frac{\delta u}{\delta t} = \nu \frac{\delta^2 u}{\delta t^2} \tag{2.5}$$

Derive exact solution for the velocity profile:

$$U = U_0 \left(1 - erf\left(\frac{y}{2\sqrt{\nu t}}\right)\right) \tag{2.6}$$

where erf is the error function.

The boundary layer thickness can be approximated by.

$$\frac{\delta u}{\delta t} = \nu \frac{\delta^2 u}{\delta t^2} \rightarrow \frac{U_0}{t} \approx \nu \frac{U_0}{\delta^2} \rightarrow \delta \approx \sqrt{\nu t} \tag{2.7}$$

The flow accelerate in the convergence zone; as flow goes faster, it reduces it pres-

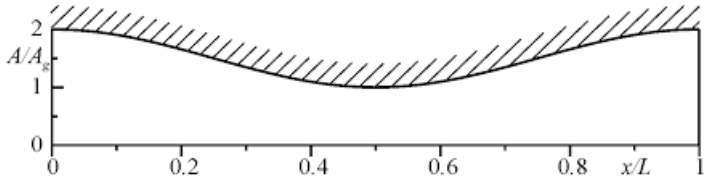

Figure 2.4: Convergence-Divergence Nozzle

sure. Flow reach maximum speed and minimum pressure at throught (minimum section). In the divergence zone he starts to decelerate to enviroment conditions. Flow goes from a lower pressure zone to an higher. Pressure gradient will be trying to slow the flow down which is exactly what we're seeing, the problem is that if the adverse pressure gradient is too hight it will slow the boundary layer too much, the presure gradient have enough force forcing the flow back that way that the boundary layer will try to return back, this causes our velocity look like (S3), which is essentially a recirculation region which is stall and this is caused by the adverse pressure gradient that pushing boundary layer flow backwards.

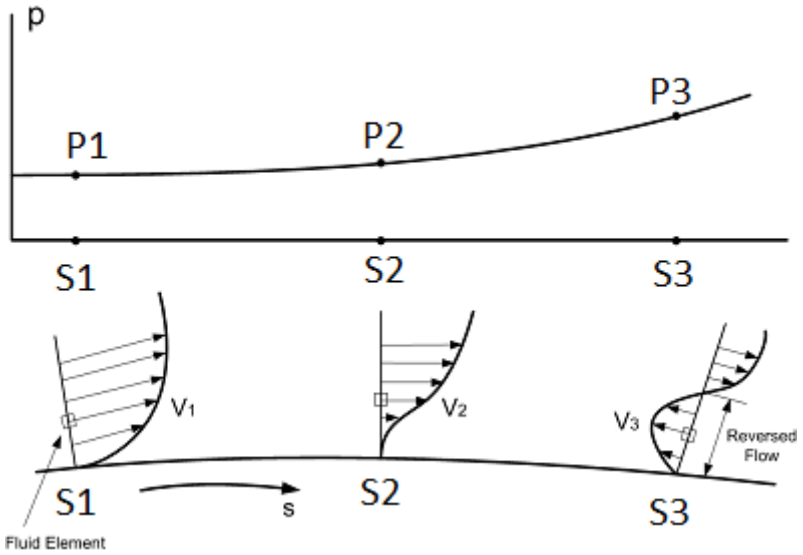

Figure 2.5: Separation Point

2.3.1 Transition Uncertainty

The prediction of boundary layer transition at assigned speeds becomes a complicated task for the aerodynamicist since the phenomenon is affected by a very large number of parameters which are difficult to determine or evaluate.[10] Indeed although the flow in the convergence zone should be laminar, the manufacturing process can affect a premature transition of the boundary layer from laminar to turbulent flow. It can be produced by the local increases of the Reynolds number. In practice how the roughness of the surface influences on the laminar to turbulent transiction isn't easy to determinate even if roughness is "a priori" known. Boundary layer transition depends on many coupled parameters. On design transition should usually occur symmetrically on both left and right sides of the vehicle, but the many parameters that influences it can cause premature transition. Laminar-turbulent transition unites two types of uncertainty. The first one is a random uncertainty ("the stochastic uncertainty") that is associated with inherent variations in the physical system or its environment. The body's smooth windward surface after repeated use or shots, might eventually become a continous pattern of asperities that could lead a premature transition to turbulent flow. The second type of uncertainty is the result of the lack of knowledge that arises from the use of inadequate physical models. Since there is no universal value for the transitional Reynolds number ReT, the inherent uncertainty in predictions that results from the evaluation of this parameter, for instance through correlations such as 2.8, needs to be be quantified in order to obtain a measure of the robustness of the design process.

$$\log_{10}(Re_T) = 6.421 exp(1.209 \cdot 10^{-4} M_{edge}^{2.641}) \tag{2.8}$$

Chapter 3

STAR-CCM+

STAR-CCM+ (Simulation of Turbulent flow in Arbitrary Regions - Computational Continuum Mechanics) is a software for computational fluid dynamics analysis (CFD), based on finite element method (FEM).

3.1 Finite Element Method

The Finite Element Method (FEM) is a numerical method based on the integration of partial differential equations on a volume control in which are established boundary solution. The total domain is divided into a collection of elementary volumes, the differential equation are calculated on any of this elementary volumes resulting in a system of algebraic equations that are be solved by calculator. The subdivision of a whole domain into simpler parts has several advantages: a better accurate representation of complex geometry, an easy representation of the total solution and the possibility to capture of local effects.
A simple cylinder body with a bad mesh loses its property.
Analyzing a bad meshes body there will be unphysics solutions. The simulator software runs anyway but it is in the user's ability to analyze results and validate them.

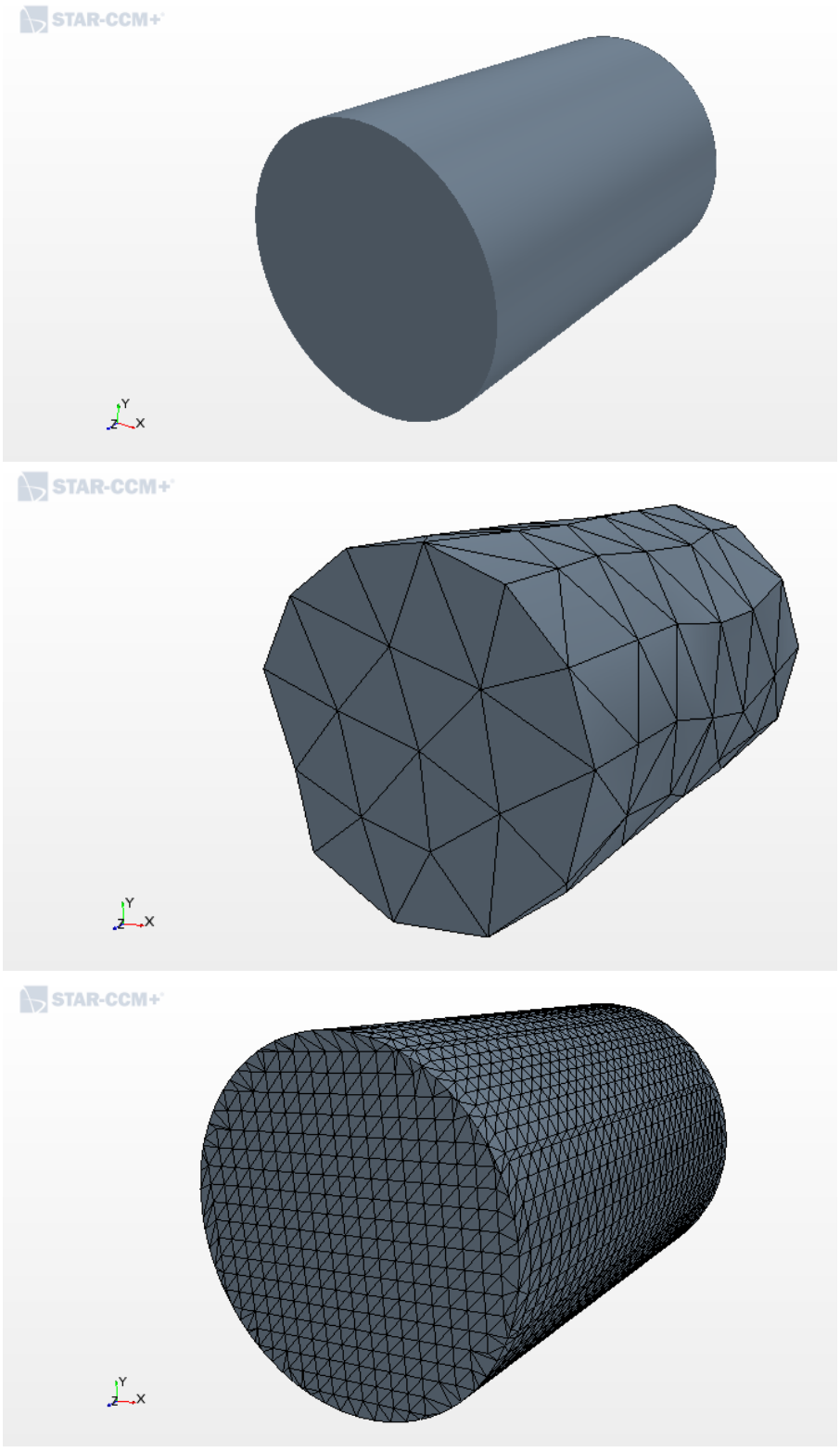

Figure 3.1: Geometry Body - Bad Mesh - Good Mesh

3.2 Geometry

3.2.1 CAD-Models: B-2019

A solid of revolution is obtained by rotating a plane figure in space about an axis coplanar to the figure. Axissymmetric body means that almoust two of its three principal moments of inertia are equal. The starting body used in this thesis (B-2019) is characterized by 8 parameters, increased to 10 improving mesh rapresentation. The 10 parameters are:

Parameter	Symbol	[m]	Fixed
Pedals Position	PP	0.64	☑
Maximun Diameter Position	MDP	1.1	☐
Shoulders Position	SP	1.74	☑
Inflection Position	IP	1.85	☐
Cut Position	CP	2.55	☐
Total Lengh	L	2.60	☐
Pedals Diameter	PD	0.227	☑
Maximum Diameter	MD	0.25	☐
Shoulders Diameter	SD	0.18	☑
Inflection Diameter	ID	0.15	☐

Table 3.1: B-2019 Parameters

Values are taken from Tarurus CAD Model. In order to guarantee necessary cyclist's comfort, are fixed three parameters: Pedals & Shoulders Positions, Pedals Diameters and Shoulders Diameter. In particuar, during optimization, pedals position and shoulders one are not fixed separately, they are related by their distance, PP and SP could translate but their distance will be unchanged (1.1 m). The same speech goes for total lengh: 5 cm far away from CP.

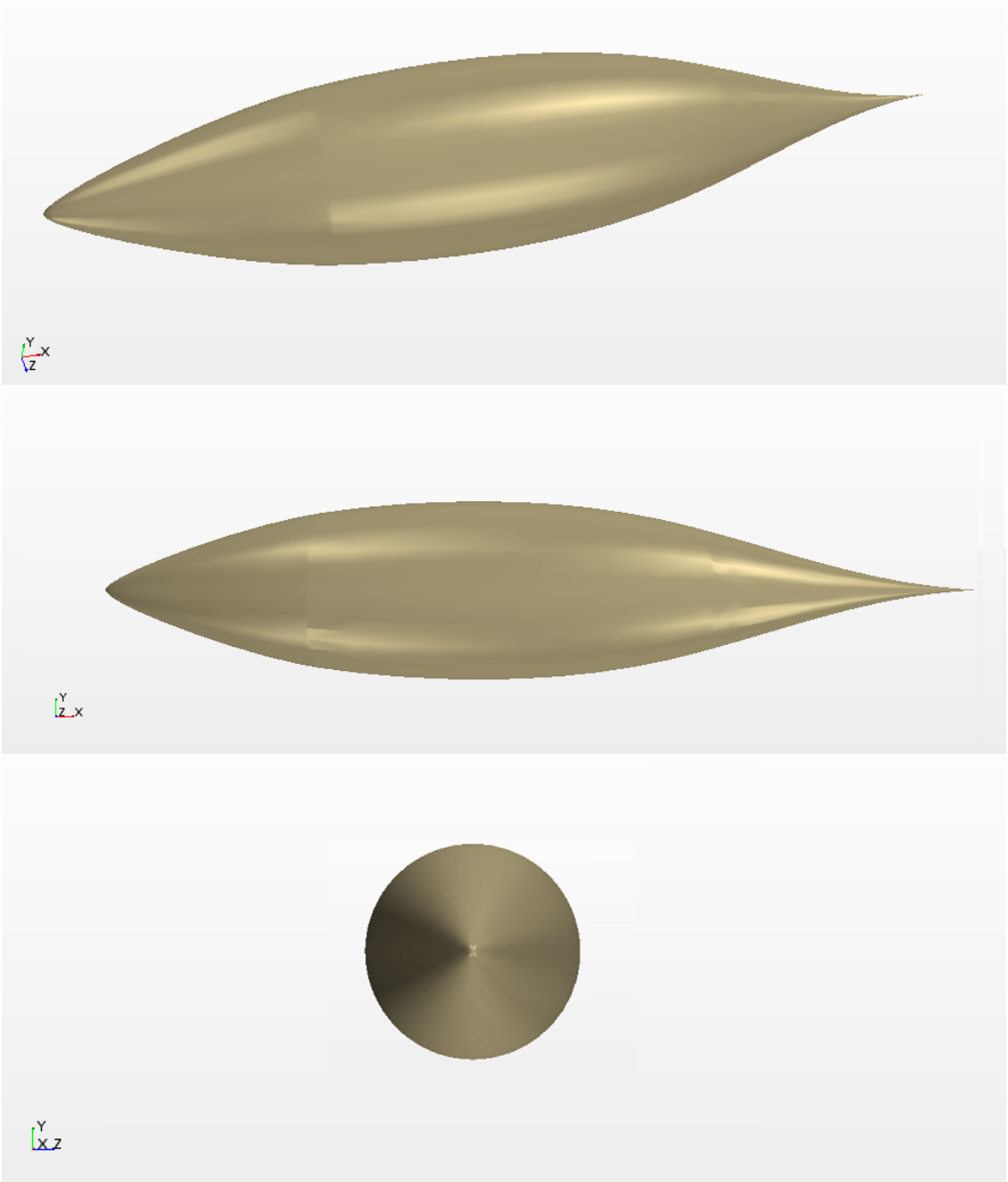

Figure 3.2: B-2019 Front and Top Views

3.2.2 Gallery

CAD-Model is located in a 3D solid that acts like a wind gallery.

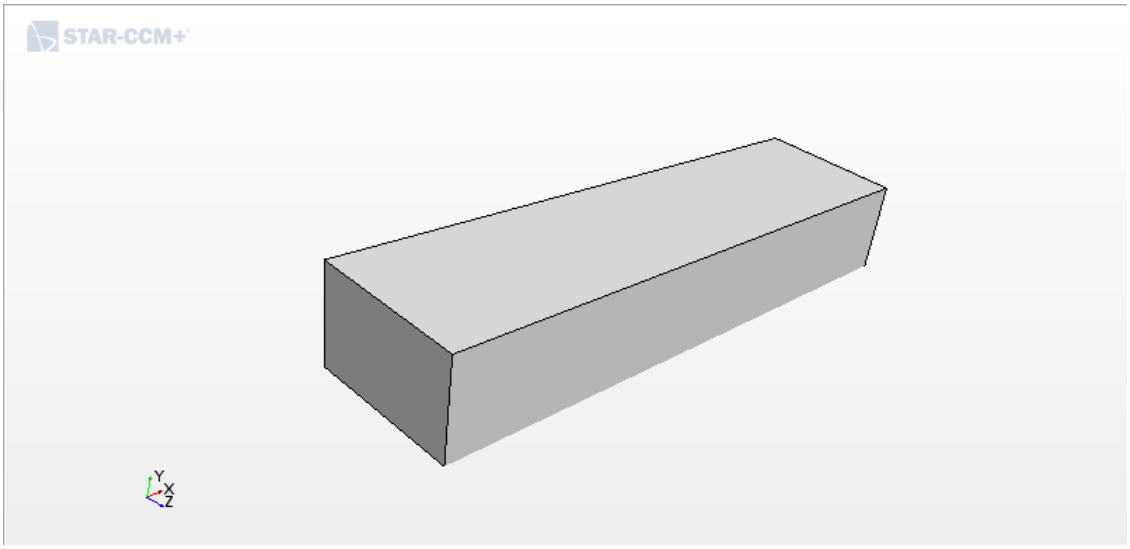

Figure 3.3: Wind Gallery

Wind gallery is big enough to let a flow natural motion.
Through Boolean operation B-2019 is subtract to the gallery. In this way the

Axis	[m]
X	30
Y	8
Z	4

Table 3.2: Gallery Dimensions

simulator software analyze the total volume whitout any solid part, since we are non interested to what happen inside the nondeformable body.

3.3 Physics Condition

3.3.1 All y+ Wall Treatment

Walls are a source of vorticity in most flow problems of practical importance. Therefore, an accurate prediction of flow and turbulence parameters across the wall boundary layer is essential. The inner region of the boundary layer can be split up into three sublayers. In each of them the flow has different characteristics and can be modeled using different empirical approaches:

- Viscous sublayer: The fluid layer in contact with the wall is dominated by viscous effects and is almost laminar. The mean flow velocity only depends on the fluid density, viscosity, distance from the wall, and the wall shear stress.

- Log-law layer: The turbulent log-law layer is dominated equally by viscous and turbulent effects.

- Buffer layer: The buffer layer is a transitional layer between the viscous sublayer and the log-law layer.

The non-dimensional wall distance can be used to define the extents of the sublayers. The following plot shows the non-dimensional velocity as a function of across the three sublayers:

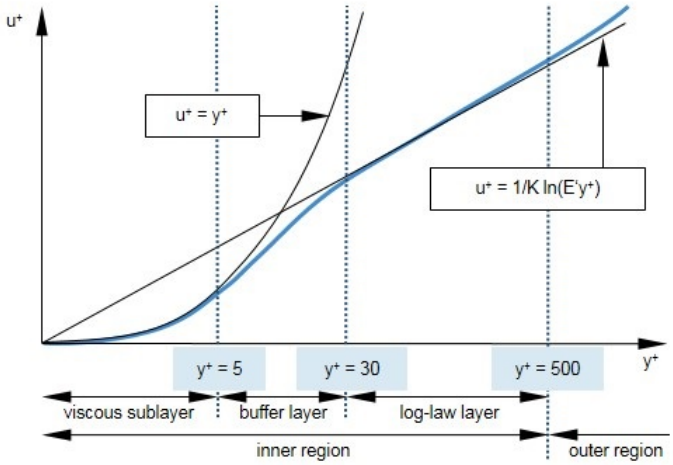

Figure 3.4: Non-dimensional velocity as a function of across the three sublayers

The low-y+ wall treatment resolves the viscous sublayer and needs little or no modeling to predict the flow across the wall boundary. The transport equations are solved all the way to the wall cell. The wall shear stress is computed as in laminar flows. To resolve the viscous sublayer, these models require a sufficiently fine mesh with near-wall cells located at of around unity. The computational expense that is associated with this approach can be significant, particularly for large Reynolds number flows where the viscous sublayer can be very thin. Therefore this wall treatment is suitable only for low Reynolds number flows.[8]

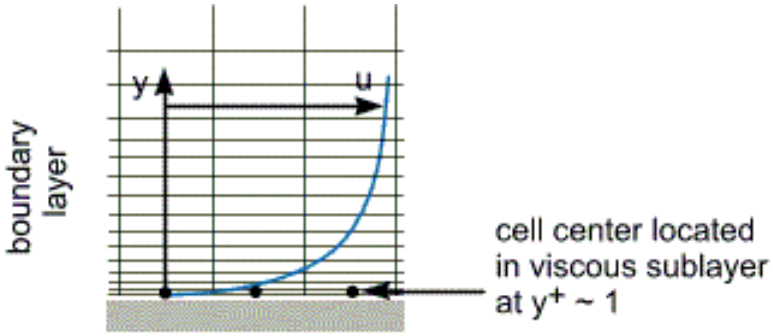

Figure 3.5: low-y+ approach

3.3.2 Gamma Re-Theta Transition Model

The Gamma Re-Theta Transition model is a two-equation correlation-based transition model that provides a true predictive capability for the onset of transition in a turbulent boundary layer.
Gamma-ReTheta Transition model allows you to solve for the turbulence intermittency γ and the transition momentum thickness Reynolds number Re_θ to predict the onset of transition in a turbulent boundary layer.

The evaluation of momentum thickness Reynolds number is avoided by relating this quantity to vorticity-based Reynolds number. In addition, a correlation for transition onset momentum thickness Reynolds number defined in the free stream is propagated into the boundary layer by a transport equation. An intermittency transport equation is further used in such a way that the source terms attempt to mimic the behavior of algebraic engineering correlations.

The Gamma ReTheta transition model is incomplete, since two critical correlations were claimed to be proprietary and hence omitted. Therefore, the model's implementation is done in such a way as to allow the custom specification of correlations via field functions. Recognizing, however, that the process of calibrating the needed correlations is complex and time consuming, the required correlations have been carefully calibrated and are provided by default within the model.

Convection	2-nd order
Cross flow term	□
Free Stream Edge	TBD

Table 3.3: Gamma ReTheta Parameters

3.3.3 Free Stream Edge

Gamma ReTheta Transiction Model needs a free stream edge function that better describes the evolution of viscous boundary layer.
This free-stream value is transported into the boundary layer through the transition momentum thickness Reynolds number Re_θ. In order to specify the value of Re_θ using a correlation, the location of the free-stream edge must be defined.
Since there is no completely general way to define the free stream, it is up to the user to create a user field function that suitably defines the free stream in such a way that the field function takes the value of 1 in the free stream and 0 inside the boundary layer. A good starting point for this definition is in terms of Wall Distance.
An example would be:

$$\$WallDistance > 0.005 \tag{3.1}$$

where it is estimated that the boundary layer is everywhere thinner than 5 mm. The user field function, once defined and named, must then be assigned to the Free Stream Edge property of the Gamma ReTheta transition model.[8] In order to formulate the function that STAR-CCM+ uses, has been analyzed a 13 inches specimen.

X	r [in]	X	r [in]	X	r [in]	X	r [in]
0	0	0.9	0.5293	5.8	1.3164	9.45	0.7346
0.001	0.0163	1	0.5614	6	1.3243	9.5	0.712
0.002	0.0231	1.2	0.6218	6.2	1.3284	9.55	0.6894
0.004	0.0327	1.4	0.6781	6.4	1.3317	9.6	0.6667
0.006	0.04	1.6	0.7308	6.6	1.3332	9.65	0.644
0.008	0.0462	1.8	0.7805	6.666	1.3333	9.7	0.6215
0.01	0.0517	2	0.8274	6.8	1.3329	9.75	0.5994
0.015	0.0634	2.2	0.8717	7	1.3297	9.8	0.5778
0.02	0.0732	2.4	0.9136	7.2	1.3225	9.85	0.5569
0.025	0.0819	2.6	0.9532	7.4	1.31	9.9	0.5368
0.03	0.0898	2.8	0.9907	7.6	1.291	10	0.4994
0.04	0.1037	3	1.0259	7.8	1.2645	10.1	0.4663
0.05	0.1161	3.2	1.0592	8	1.23	10.2	0.4378
0.06	0.1273	3.4	1.0904	8.2	1.1868	10.3	0.4141
0.07	0.1377	3.6	1.1196	8.4	1.1348	10.4	0.3953
0.08	0.1474	3.8	1.1468	8.5	1.1055	10.5	0.3811
0.09	0.1565	4	1.1722	8.6	1.074	10.6	0.3713
0.1	0.1651	4.2	1.1956	8.7	1.0404	10.7	0.3654
0.2	0.2359	4.4	1.2172	8.8	1.0048	10.8	0.3629
0.3	0.2917	4.6	1.2369	8.9	0.9673	11	0.3659
0.4	0.3399	4.8	1.2547	9	0.928	11.2	0.3752
0.5	0.3832	5	1.2707	9.1	0.8872	11.4	0.3861
0.6	0.4232	5.2	1.2849	9.2	0.8449	11	0.3947
0.7	0.4605	5.4	1.2972	9.3	0.8015	11.8	0.3992
0.8	0.4958	5.6	1.3077	9.4	0.7571	12	0.4

Table 3.4: 13-Inches Profile Plot Data

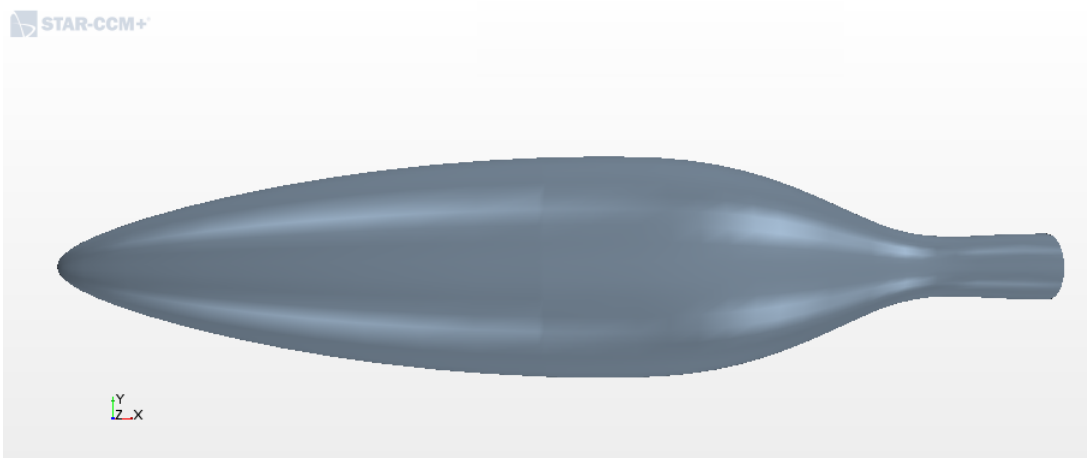

Figure 3.6: 13-in Profile

The field function that better revive 13 inches speciment experimental results is:

$$\frac{V^2}{2 \cdot \frac{(p_{ref}-p_0)}{\rho_{ref}} + S^2} > 0.9801 || W_D > W_{Dmax} \tag{3.2}$$

Where:

- V (Velocity) is the elementar cell local speed
- S (Speed) is the reference speed (150 kph)
- ρ=ρ_{ref} since constant density model
- p_{ref} is the reference pressure (101 325 Pa)
- W_D is the elementar cell distance from the wall

The function study boundary layer from Bernoulli's principle.

$$\frac{1}{2}\rho V^2 + p = cost \tag{3.3}$$

Specialized for viscous region it becomes:

$$\frac{1}{2}\rho V^2 + p = \frac{1}{2}\rho_{ref}(99\% \cdot S)^2 + p_{ref} \tag{3.4}$$

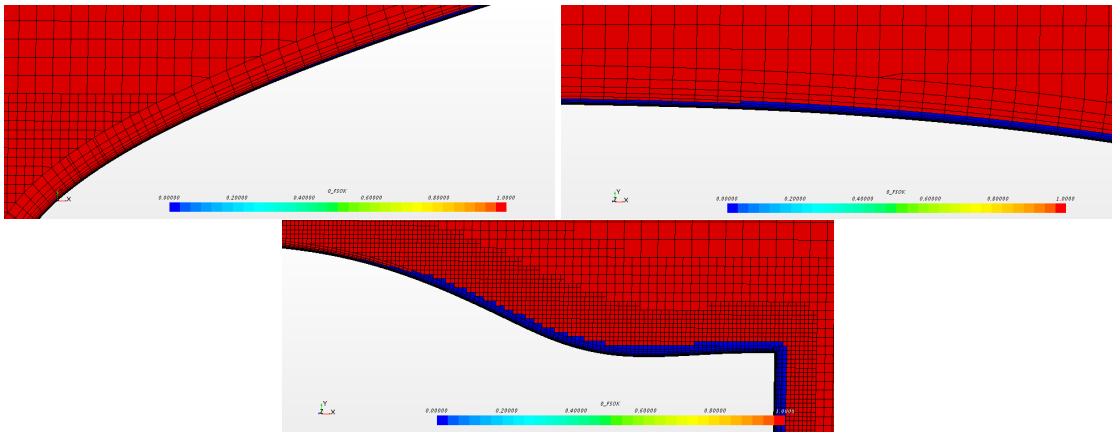

Figure 3.7: Field Function

According to experimental results, Star-CCM+ Drag Coefficient and Experimental drag coefficient are above 0.04. Also, through Wall Shear Stress analysis, it could be possible extimated transiction point. Both Experimental and Star-CCM+ points are above the 60% of the total length. [9]
Analyzing the Field Function is possible to notice its trend. It star from zeros, or little more, at the nose till reach 16 mm at the profile ending point. This assignment is phisically correct since field funtion isn't costant across the body like starting function allowed to understand.

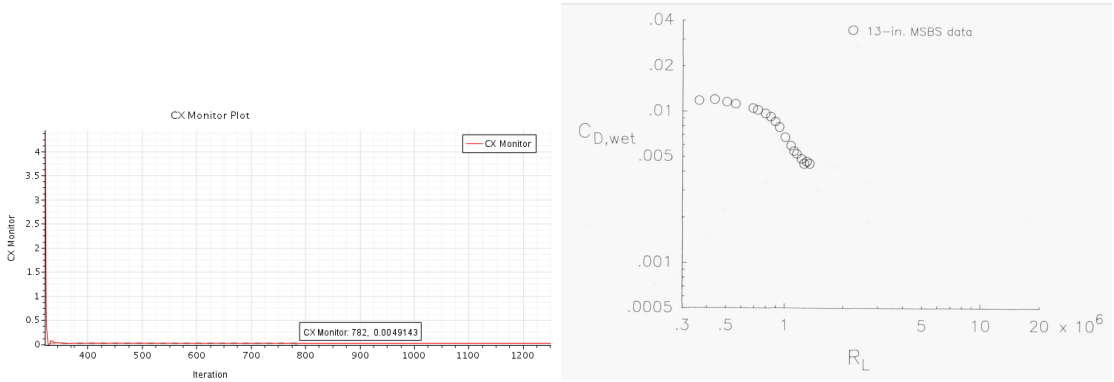

Figure 3.8: Star CCM+ Drag Coefficient vs Experimental CD

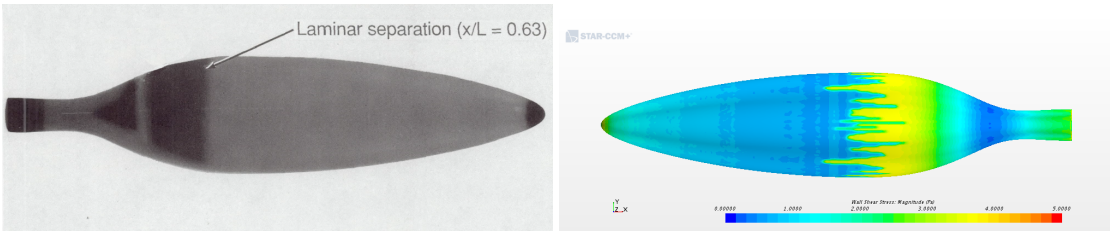

Figure 3.9: Liquid crystal flow vs Star CCM+ visualization for free transition. Re=1.2E6

3.3.4 Wall Shear Stress

Figure 3.9 represents the Wall Shear Stress (τ_w) on 13-inches speciment.
It is the component of stress coplanar with a material cross section. Shear stress arises from the force vector component parallel to the cross section of the material. Any real fluids moving along a solid boundary will incur a shear stress at that boundary. The no-slip condition dictates that the speed of the fluid at the boundary (relative to the boundary) is zero; although at some height from the boundary the flow speed must equal that of the fluid. For all Newtonian fluids in laminar flow, the shear stress is proportional to the strain rate in the fluid, where the viscosity is the constant of proportionality. The shear stress is imparted onto the boundary as a result of this loss of velocity.

For a Newtonian fluid, the shear stress at a surface element parallel to a flat

plate at the point y is given by:

$$\tau(y) = \mu \frac{\partial u}{\partial y} \tau(y) = \mu \frac{\partial u}{\partial y} \tag{3.5}$$

Where:

- μ is the dynamic viscosity of the flow;
- u is the flow velocity along the boundary;
- y is the height above the boundary.

Specifically, the Wall Shear Stress is given by:

$$\tau_w = \mu \left(\frac{\delta u}{\delta y} \right)_{y=0} \tag{3.6}$$

It plays a significant role in transiction point's analysis. When it value start to become higher means that lamimar to turbulent transiction process starts, viscous boundary layer become more unstable until the detachment from the body.
The SI unit of wall shear stress is pascal (Pa), which is identical to $\frac{kg}{m \cdot s^2}$.

3.3.5 Cell Quality Remediation

The Cell Quality Remediation model helps you get solutions on a poor-quality mesh. This model identifies poor-quality cells, using a set of predefined criteria, such as Skewness Angle exceeding a certain threshold. Once these cells and their neighbors have been marked, the computed gradients in these cells are modified in such a way as to improve the robustness of the solution.In general, the effect of Cell Quality Remediation is confined to the immediate vicinity of poor-quality and/or degenerate cells, so that the influence on overall solution accuracy is minimal.[8]

3.3.6 Exact Wall Distance

The Exact Wall Distance model makes an exact projection calculation in real space, which is based on a triangulation of the surface mesh. The use of K-D search trees or SFC/SIMD algorithms accelerates the calculation.
The Exact Wall Distance model is selected on your behalf after the selection of a specific physical model that requires the wall distance parameter.[8]

3.3.7 Gas

Gas used is Air in standard conditions.

Air	
Density	$1.225\,\mathrm{kg/m^3}$
Dynamic Viscosity	$1.8 \times 10^{-5}\,\mathrm{Pa \cdot s}$
Speed	$150\,\mathrm{kph}$
Pressure	$101\,325\,\mathrm{Pa}$

Table 3.5: Air Data

3.3.8 Turbulent

A flow that is in a state of continuous instability, exhibiting irregular, small-scale, high-frequency fluctuations in both space and time is termed turbulent. It is strictly possible to simulate turbulent flow directly by resolving all the scales of the flow (termed direct numerical simulation). However, the computer resources that are required are too large for practical flow simulations. Therefore, a suitable turbulence modeling approach must be selected.[8]

3.3.9 Segregated Flow

The Segregated Flow model solves the flow equations (one for each component of velocity, and one for pressure) in a segregated, or uncoupled, manner. The linkage between the momentum and continuity equations is achieved with a predictor-corrector approach.[8]
Other enabled models:

- Constant Density
- Steady
- Three Dimensional Model

3.4 Regions

Regions are volume domains (or areas in a two-dimensional case) in space that are completely surrounded by boundaries. They are discretized by a conformal mesh consisting of connected faces, cells and vertices. One region is joined to another using an interface, so that information can be passed between them. Boundaries are not shared between regions. There may be multiple regions in a simulation, each with a unique name and properties.
Region nodes are created when you:

- Import a mesh, ad exemple from native CAD
- Split a non-contiguous region
- Assign parts to regions

Creating regions from existing boundaries is possible to apply different physical properties to a portion of the fluid domain. To each region are assigned:

- Mesh Continuum
- Physics Continuum
- Parts
- Type

In the studied case there is one region and four difference boundaries:

Boundary	Type	Shear Stress Specification
(A) Inlet	Velocity Inlet	n/a
(B) Outlet	Pressure Outlet	n/a
(C) Body	Wall	No-slip
(D) Ground	Wall	Slip

Table 3.6: Boundaries

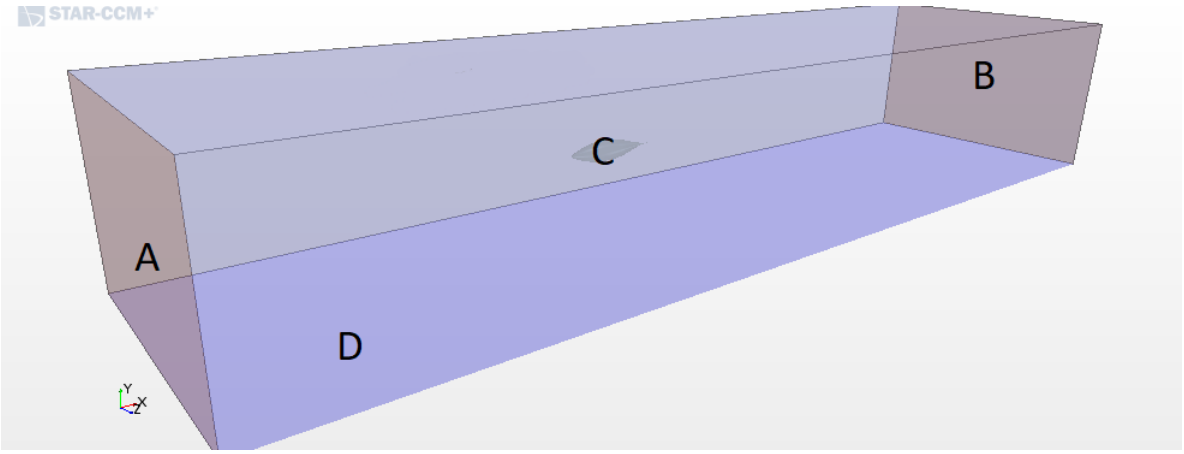

Figure 3.10: Boundaries

3.5 Mesh Conditions

The total volume is divided into 4161718 trimed elementary cells that better dscribes the geometry and physics problems. The base size for the surface mesh is 3 cm, while the volume mesh target is the 0.1% (0.01 m). There are 16 prism layers for 16 mm and the nearest layer is far 0.16 µm from the body wall. Obviously the mesh is thicker near the wall and grows away from it. Beyond the body there is a 8 meters region (across X) that analyzes the trail.

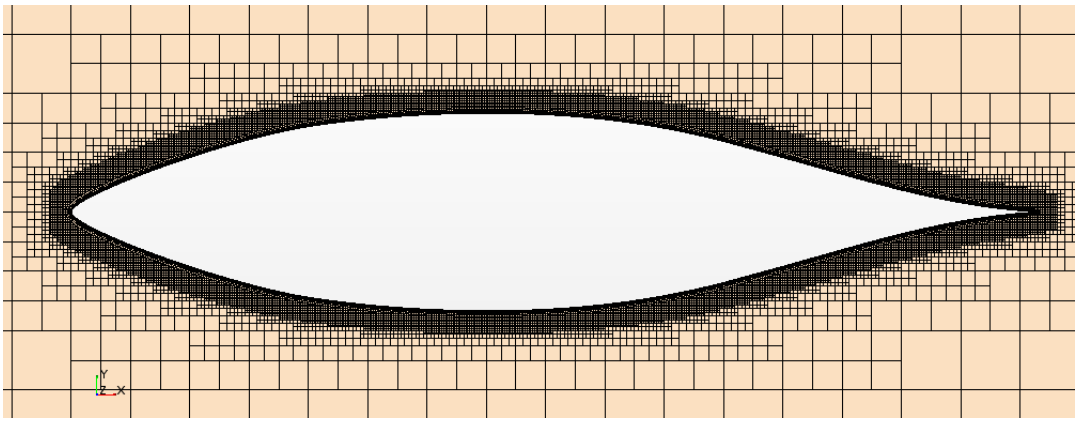

Figure 3.11: Volume Mesh

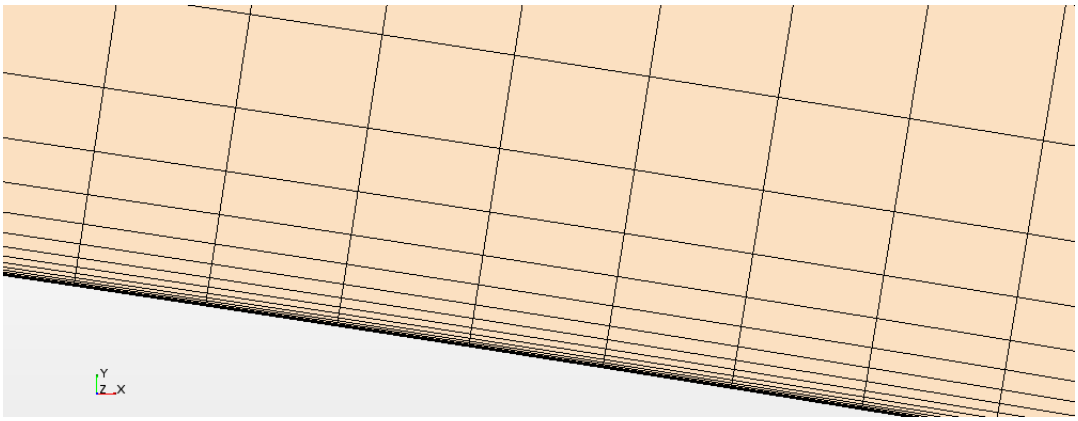

Figure 3.12: 16 Prism Layers Details

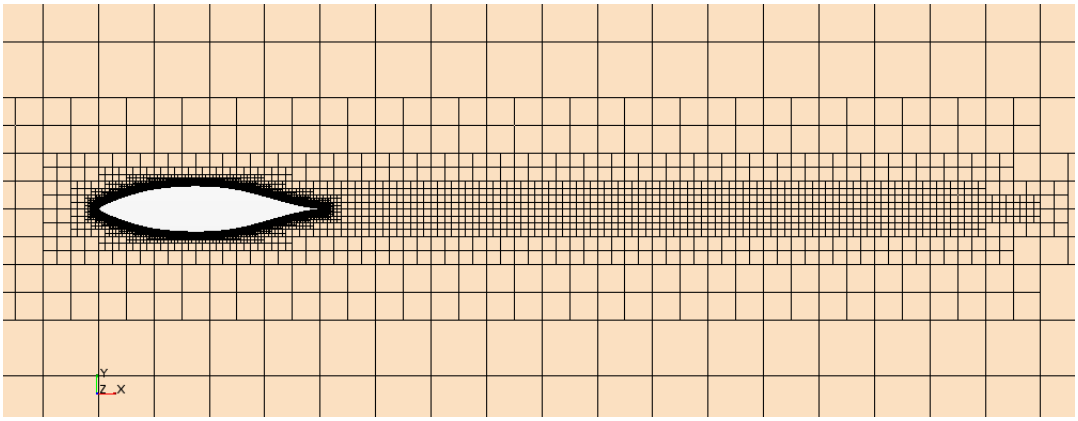

Figure 3.13: Trail Details

Controls	Values
Cells	4161718
Base Size	10 m
Target Surface Size	0.006 m
Minimum Surface Size	0.003 m
Surface Growth Rate	2.0
Auto-Repair Minimum Proximity	1.0×10^{-4} m
Prism Layer Near Wall Thickness	1.6×10^{-5} m
Number of Prism Layers	16
Prism Layer Total Thickness	0.016 m
Default Growth Rate	Fast
Surface Growth Rate	Very Slow
Distance	8 m
Wake Refinement	0.1 m

Table 3.7: Mesh Conditions

3.6 Plots and Results

Running Star-CCM+ for 1500 iterations, in order to have stationariety and convergence, the results are:

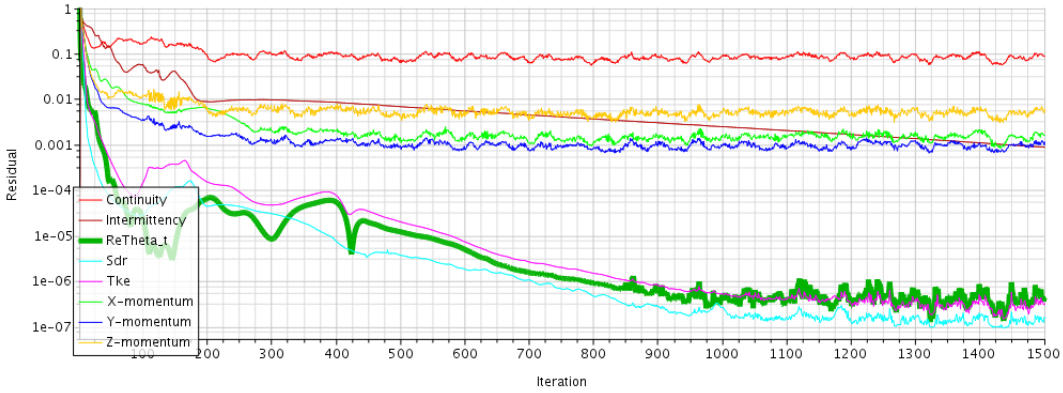

Figure 3.14: Residuals

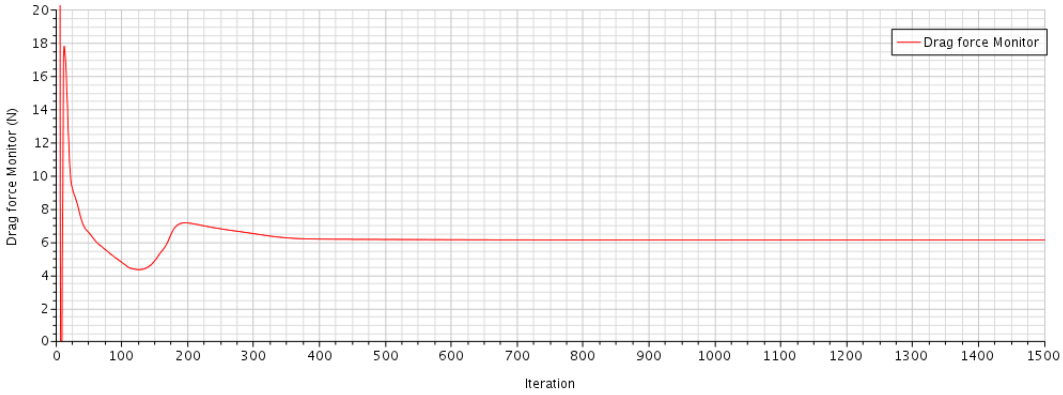

Figure 3.15: Drag

There is convergence in results since errors are settled on costant and very little values. Green curve represents Gamma Re-Theta Transition Model, that is the last residual to converge (1000 iterations).
Drag value is of 6.12 N.

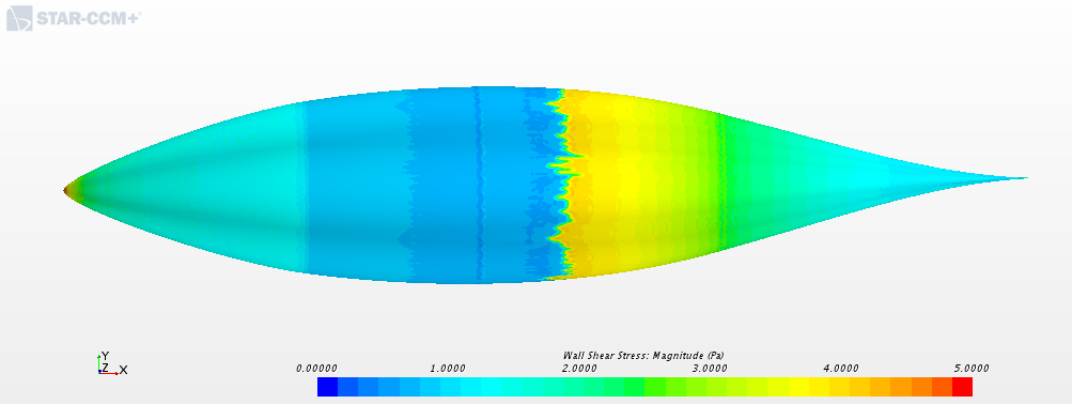

Figure 3.16: Wall Shear Stress

Thanks to WSS scene is possible to analyze transiction. It is located after the maximum diameter point, at almoust the 60% of the total lenght.

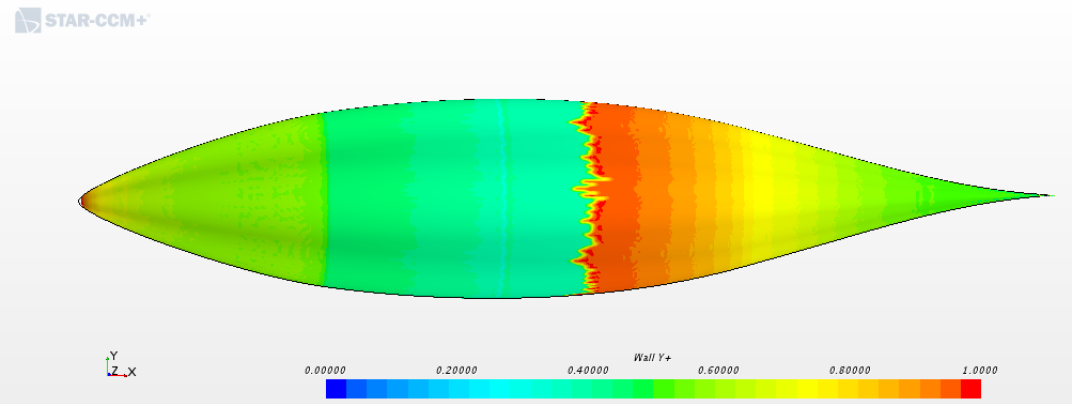

Figure 3.17: Wall-y+

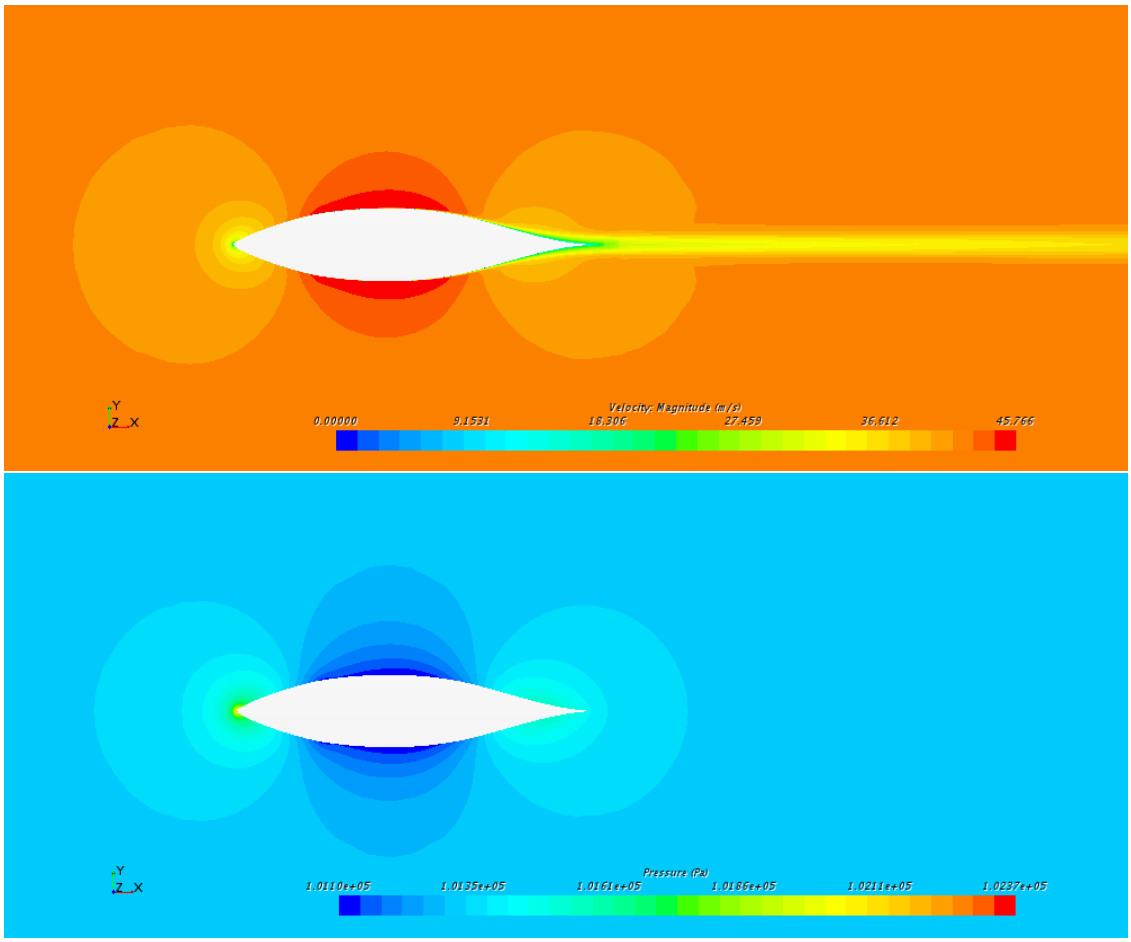

Figure 3.18: Speed and Pressure

Speed and pressure values are in according to phisycs problem. In corrispondence of profile leading edge and the ending edge, where there are two stopping points, we have maximum pressure and zero velocity. Velocity increases till its maximum (and minimum pressure) point that is located in corrispondence of B-2019 maximum diameter.

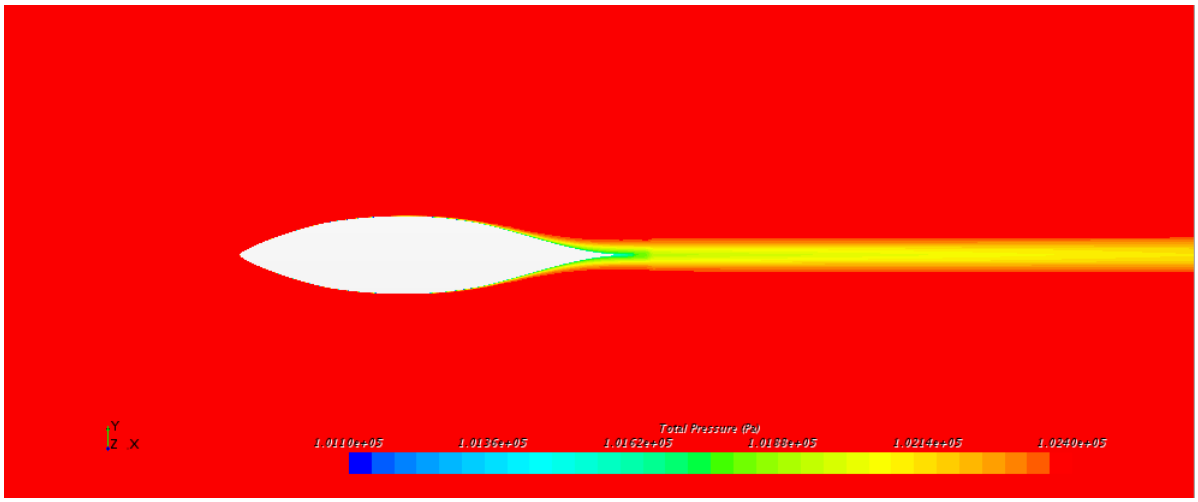

Figure 3.19: Total Pressure

The total pressure doesn't change except for numerical errors that are brought to valley by the viscousity introducted by the numerical method.
The viscosity effect causes the damping of the solutions, a small results' precision lost but makes the numerical method stable.

Chapter 4

HEEDS

The shape optimization problem is solved using HEEDS software. HEEDS allows the user to compare difference simulation results modifying design paramenters.

4.0.1 Parameters

There are 2 different classes of parameters: variables and responces.
The first ones could change their values in order to get different results; the second parameters are the mission target, what HEEDS research to accomplish the mission. The only target is to minimize the Drag Force value. Fixing pedals and shoulder's diameters and their distace, the other eight parameters could be combinated as follows:

Variable	Type	min [m]	Baseline [m]	max [m]
PP	Continuos	0.4	0.64	0.8
MDP	Continuos	0.9	1.1	1.5
SP	Dependent		PP+1.1	
IP	Continuos	1.7	1.85	2
CP	Continuos	2.4	2.55	2.8
L	Dependent		CP+0.05	
MD	Continuos	0.23	0.26	0.4
ID	Continuos	0.1	0.15	0.2
PD	Fixed		0.227	
SD	Fixed		0.18	

Table 4.1: HEEDS Parameters

4.1 Results

After analyzing over 100 parameters combinations, HEEDS established that best configurations are:

4.1.1 Design A

Variable	Value [m]
PP	0.64
MDP	1.1
SP	1.74
IP	1.81
CP	2.52
L	2.57
MD	0.26
ID	0.16
PD	0.227
SD	0.18
Drag	6.12 N

Table 4.2: Design A - Parameters

Figure 4.1: Design A - Body

The first design has a Drag Force value similar to the original shape.
This design has inflection position 4 cm forward the original design; it is 3 cm shorter and has the inflection diameter higher than B-2019. All this variation lead to a bigger curvature in order to manintain the zero grades tangency at the ending edge. Star analysis show no differences in drag force.

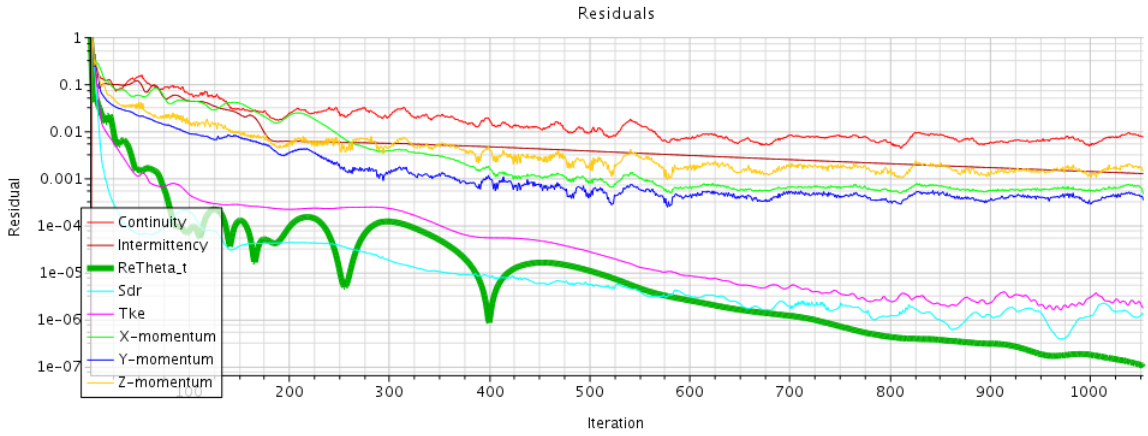

Figure 4.2: Design A Residuals

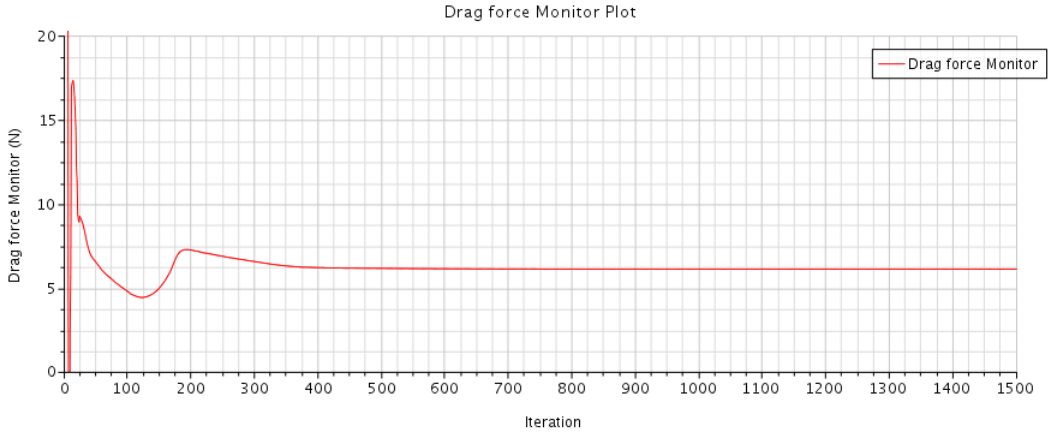

Figure 4.3: Design A Drag

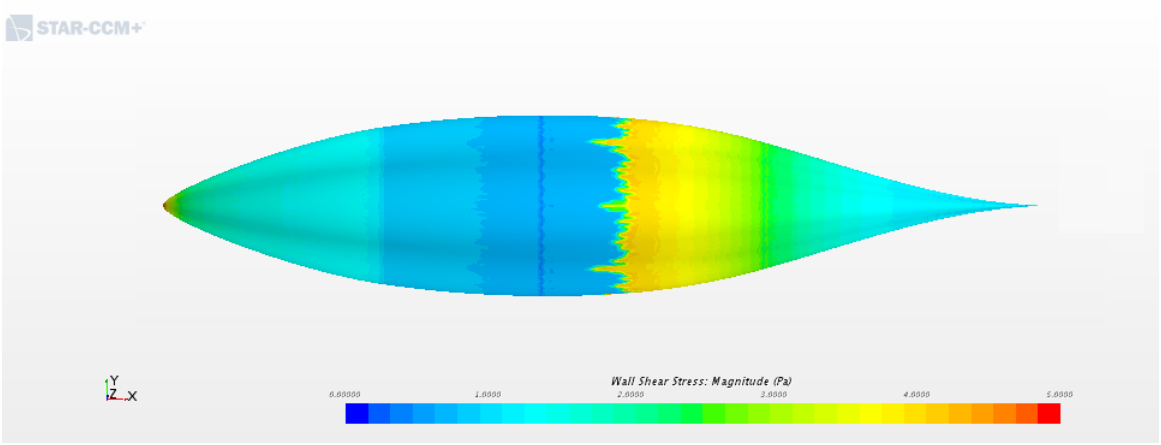

Figure 4.4: Design A Wall Shear Stress

4.1.2 Design B

Variable	Value [m]
PP	0.64
MDP	1.1
SP	1.74
IP	1.85
CP	2.53
L	2.58
MD	0.26
ID	0.16
PD	0.227
SD	0.18
Drag	6.06 N

Table 4.3: Design B - Parameters

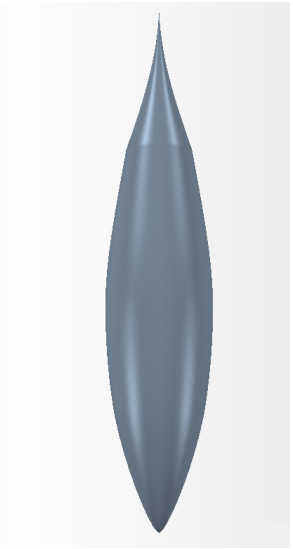

Figure 4.5: Design B - Body

Thanks this new shape drag is reduced of 1%.
There is convergence in results since residuals do not change their values during iterations; transiction point is located after maximum diameter, 1.1 m from the nose. In this way laminar flow could reach over the 60% of the total lenght.
There's not differences in speed and pressure evolution (convergence-diveregence nozzle) .
Total pressure show the usual machine error, due to truncation, and the viscosity introducted by numerical method.
A significan little difference with other shapes is the fast tangency change in the queue due to the fact that B-Design is 2 cm shorter than the original shape (keeping the other parameters unchanged).

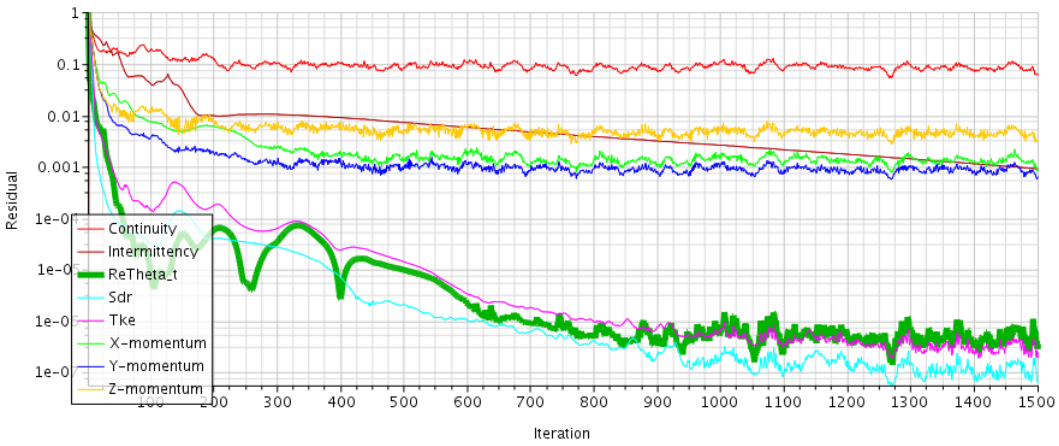

Figure 4.6: Design B Residuals

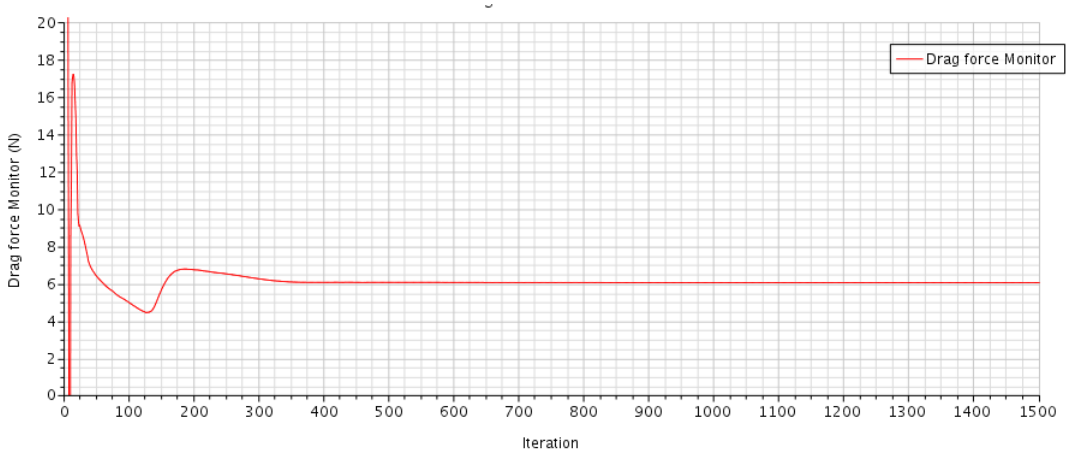

Figure 4.7: Design B Drag

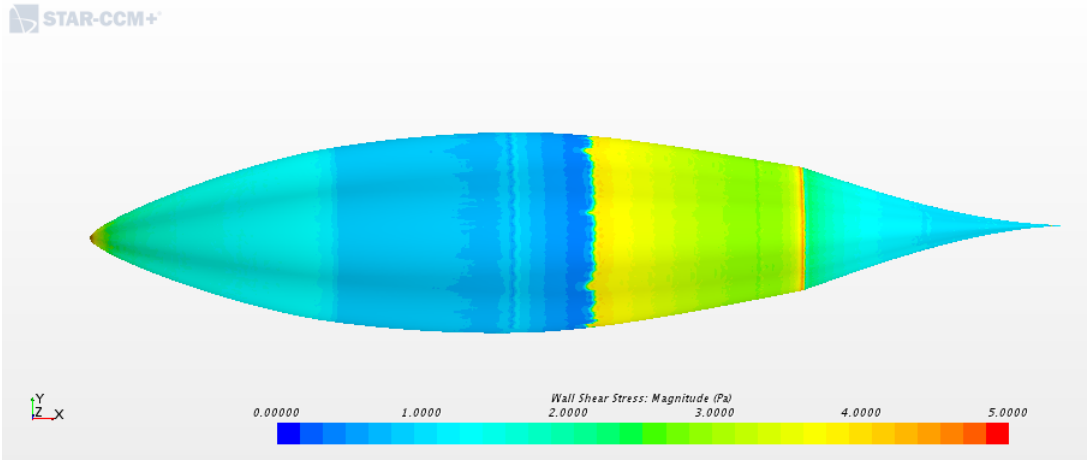

Figure 4.8: Design B Wall Shear Stress

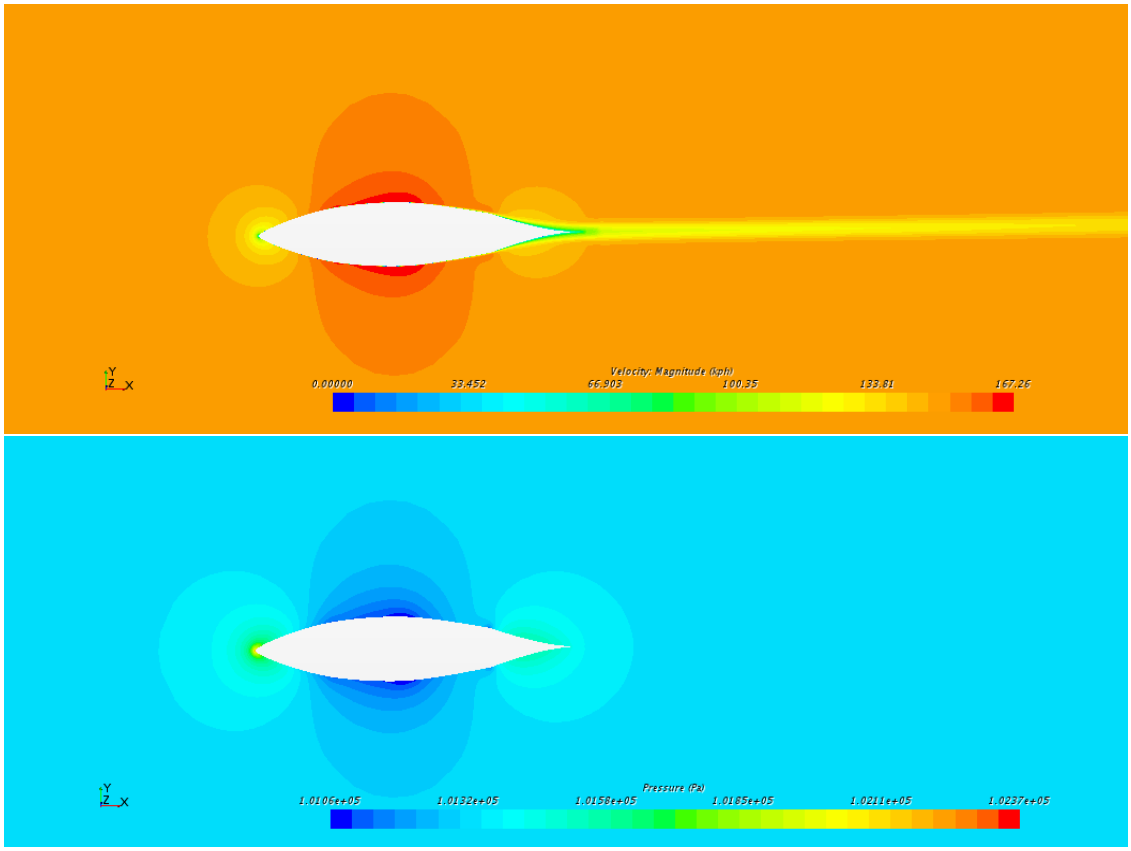

Figure 4.9: Design B Speed and Pressure

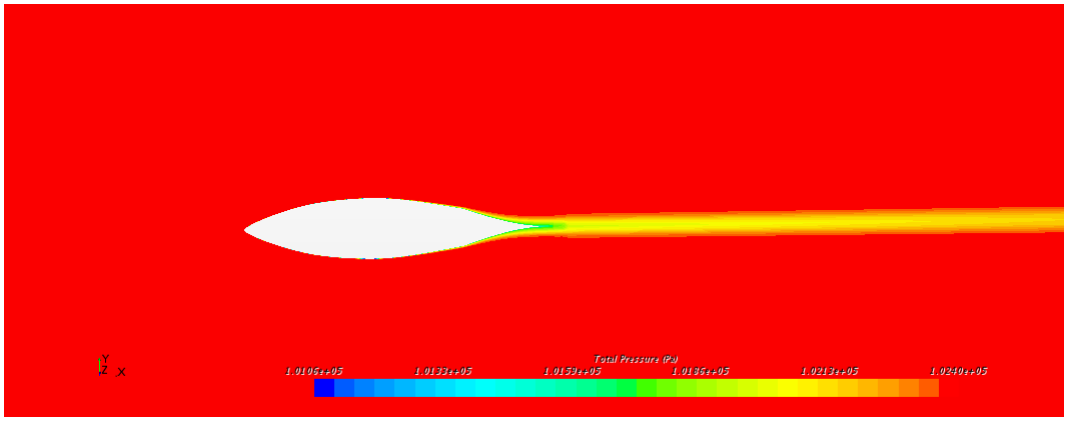

Figure 4.10: Design B Total Pressure

4.1.3 Design C

Variable	Value [m]
PP	0.64
MDP	1.1
SP	1.78
IP	1.81
CP	2.52
L	2.57
MD	0.27
ID	0.16
PD	0.227
SD	0.18
Drag	5.94 N

Table 4.4: Design C - Parameters

Figure 4.11: Design C - Body

C shape is the best Design.
In this configuration Maximum Diameter is increased by 2 mm. This could lead to a sudden detachment of laminar flow but, increasing Inflection Diameter and its approach to the shoulder position (4 mm nearest), speed flow increases softly and laminar flow grows more in the divergence zone, a determinant variation for the reduction of aerodynamic drag.
It is 3 cm shorter than B-2019 Design.
Speed, pressure and total pressure doesn't show any particular differences from other solutions, while the total pressure show the usual viscosity effect.

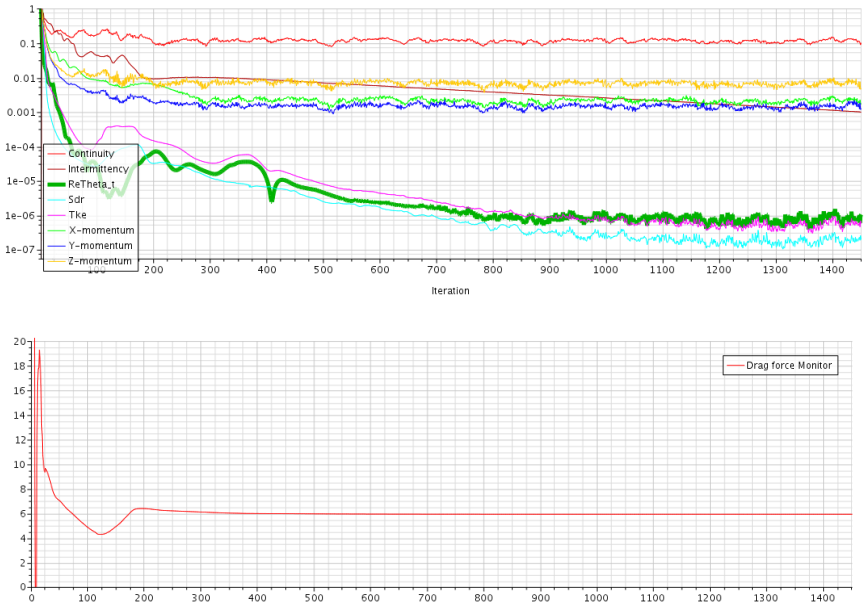

Figure 4.12: Design C Drag and Residuals

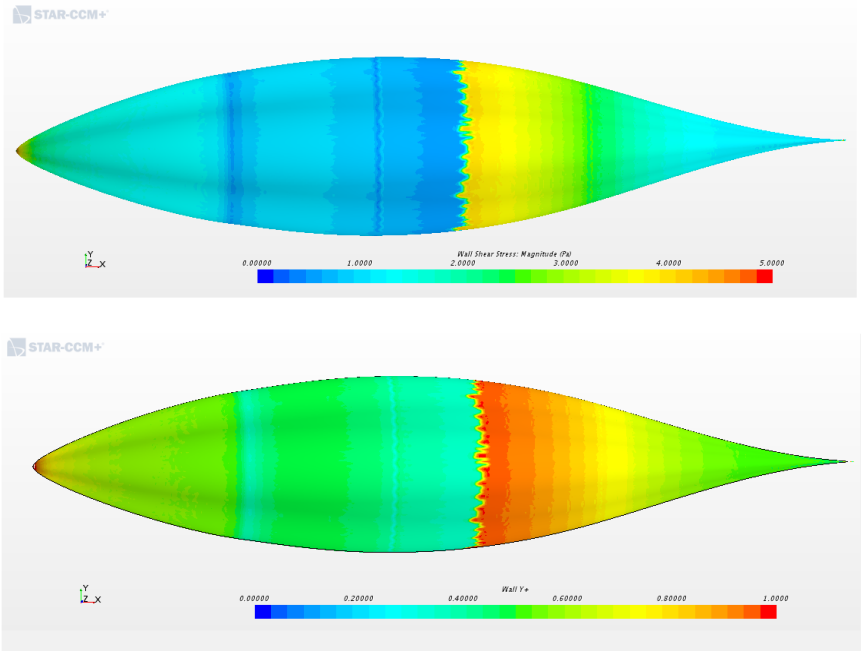

Figure 4.13: Design C WSS and Wally+

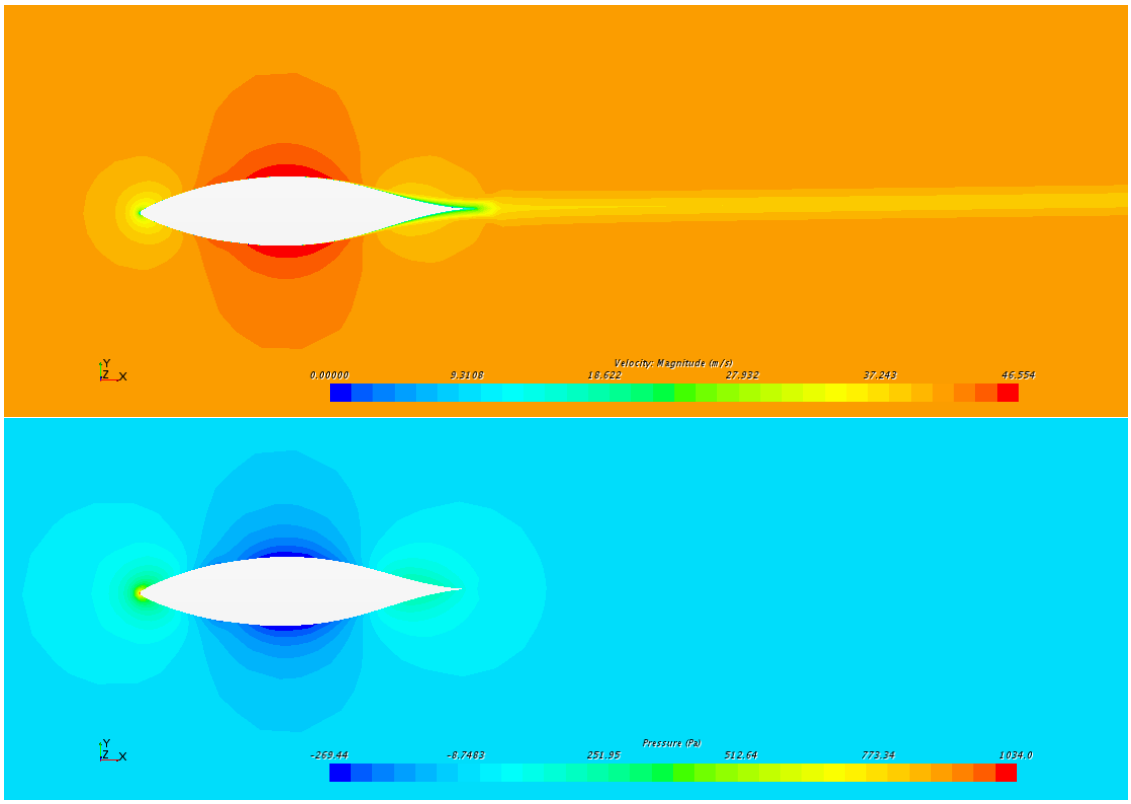

Figure 4.14: Design C Speed and Pressure

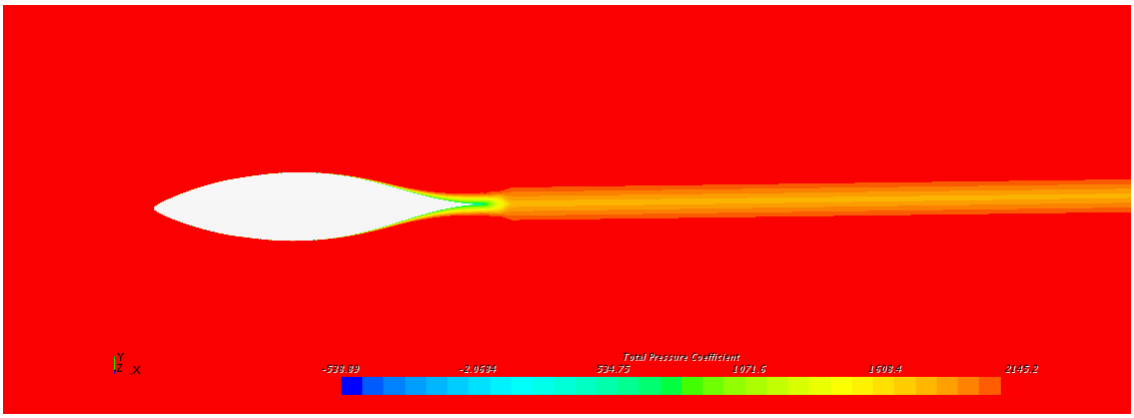

Figure 4.15: Design C Total Pressure

Even there is a little difference in the input parameters, HEEDS result gives better performance and an almoust 3% drag decrease.

Body	Drag [N]	
B-2019	6.12	
Design A	6.12	0 %
Design B	6.06	-1.0%
Design C	5.94	-2.93%

Table 4.5: Design Comparison

C-Design is the best shape at given Reynolds and speed. In the following study we consider this best design as the default one.

Chapter 5

Ground Effect

In the previous chapter B-2019 study was carried out in air, the body has been placed at a distance from the boundaries that let the normal trend flow. In this chapter B-2019 will be near to the ground in order to consider Ground Effect.
In computational analysis term it means to aplly no-slip condition to the wall, the flow adheres to it. Viscous boundary layer must be considered also on the ground; there flow speed is zero, it grows away from te wall till the 99% where boundary layer ends. In order to describe better this phenomenon will be add, to the original mesh, 16 prism layers to the ground.

Boundary	Type	Shear Stress Specification
(A) Inlet	Velocity Inlet	n/a
(B) Outlet	Pressure Outlet	n/a
(C) Body	Wall	No-slip
(D) Ground	Wall	No-slip

Table 5.1: Region Boundaries Condition

There are two modes to analyze it. In the first mode B-2019 original shape is slightly modified with addition of two "wheels", in the second mode the wheels were removed since they have a less important role in drag foce computation.

5.0.1 With Wheels

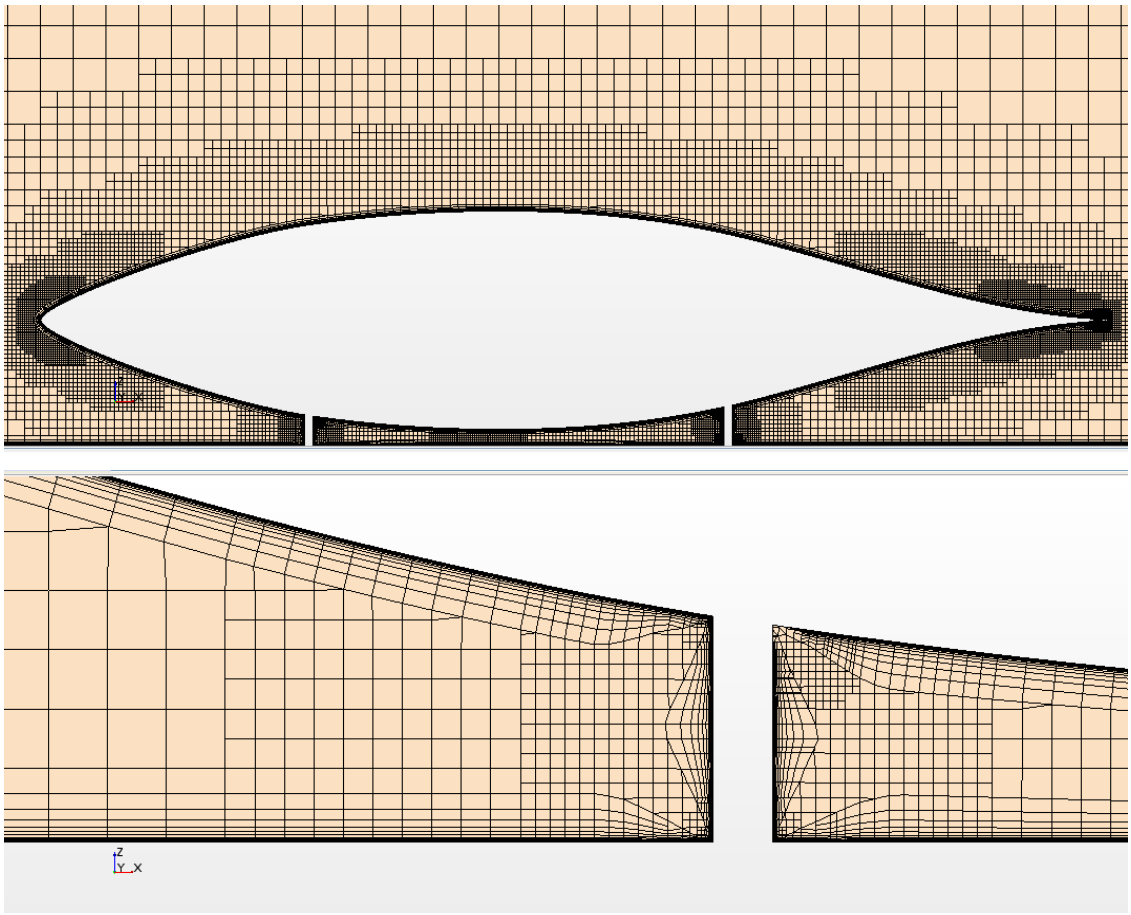

Figure 5.1: Ground Prism Layer Volume Mesh

As previously said body shape is modified. To the original body have been added two cylinders, that represents the two wheels. Volume mesh count 4761321 cells since it has improved in corrispondence of the cylinders and the ground.
Adding two cylinders we lost the axissymetric geometry shaoe of the original body.

Running Star-CCM+ for 1300 iterations, in order to have stationary and convergences solutions, the results are:
Drag value is of 6.58 N

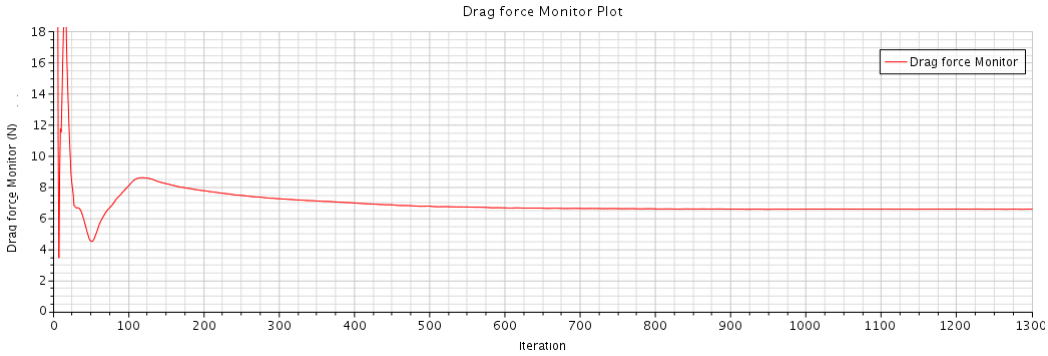

Figure 5.2: GE Drag

This value is very close to B-2019 Drag Force value. With this results wheels influence on drag force is very small on the total value. In this way in the next section is analyzed a no-axissymetric body without wheels.

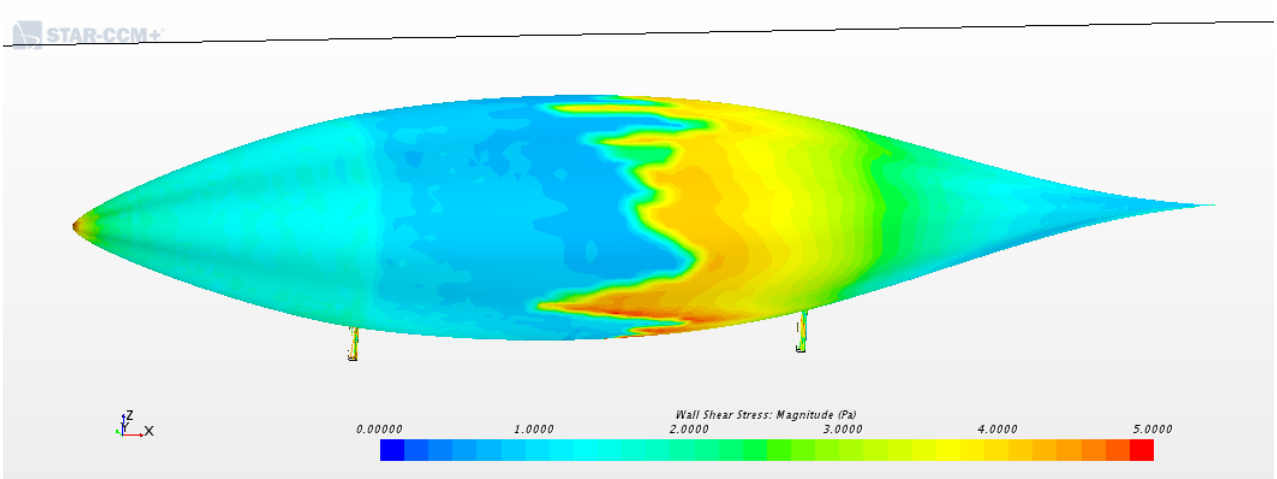

Figure 5.3: GE Wall Shear Stress

From WSS it could be possible analyze transiction point. It is located after the maximum diameter points, at almoust the 60% of the total lenght.

Speed and pressure values are in according to the phisycs problem. Maximum pressure at the leading edge and at the end, where there are two stopping points;

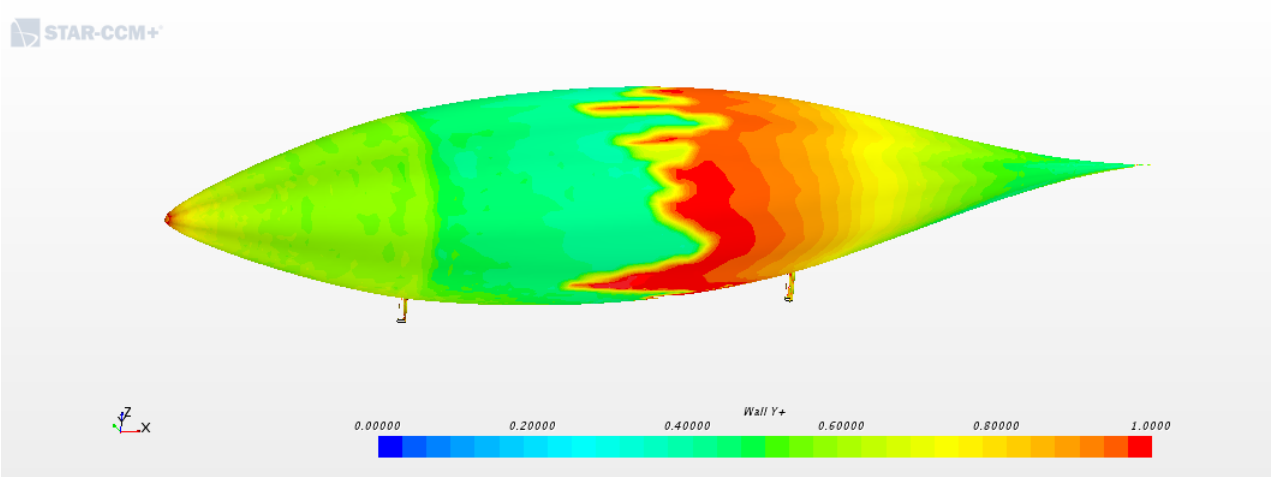

Figure 5.4: GE Wall-y+

maximum speed and minimum pressure point is located in corrispondence of B-2019 maximum diameter. Total pressure doesn't change except for numerical errors that are brought to valley by the viscousity introducted by the numerical method.

5.0.2 Whithout Wheels: No Axissymmetric Body

The second way to analyze groud effect is possible thanks to the little effect of the wheels to the drag force value.
In this study the body is no more an axissymetric one but it is created with a loft operation between four splines.

Each spline is bound to go through pedals, maximum, shoulders and inflection

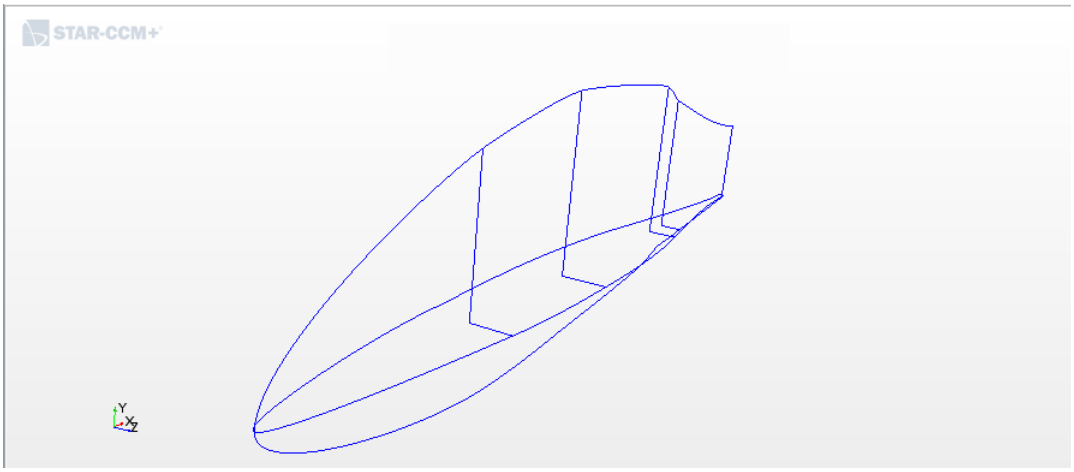

Figure 5.5: Four Splines

positions. Also they are tangent 90 grades to the nose.
X cordinates are set up on HEEDS best optimization design: C-Design. The optimation process will study the effect of top curvature due to the different bike heights at pedals, maximum diameter and shoulder position.
Reports show that it is better to have a bicycle where the difference between heights is very small compared to the actual height. Difference between pedals and shoulders height must be smaller than 20 cm, with an 8° curvature. Top height and shoulders one must be similar (3∼5 cm)

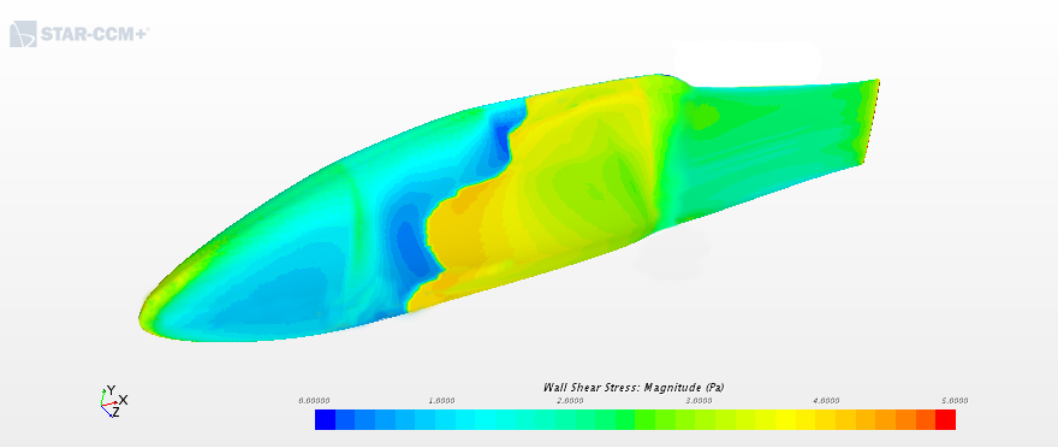

Figure 5.6: No AXB WSS

Wall Shear Stress show how laminar separation appear first on the body side and later on the top. This is caused by on top, the curvature is bigger than the side one. While the flow across the top has a favourite gradient pressure, on the body side the particelles already enters in the adverse gradient pressure zone.

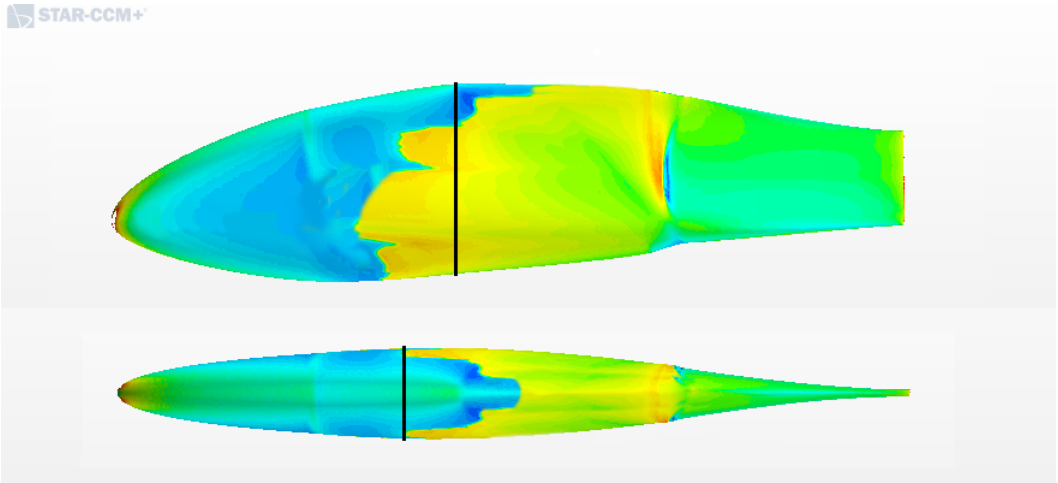

Figure 5.7: Maximum Diameters

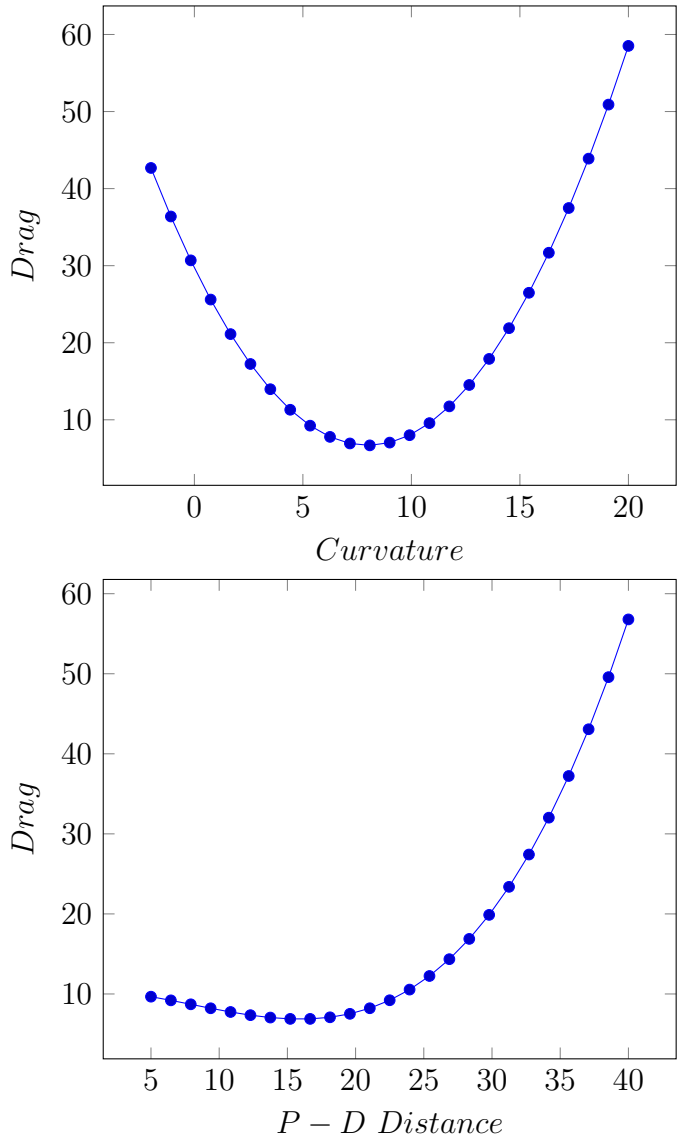

This graphics show the previous discusses results.The difference between pedals and shoulders height must be smaller than 20 cm, with an 8° curvature. The difference between height and shoulders heigh must be very small (3∼5 cm).

Chapter 6

Summary and Outlook

The present work illustrates shape optimization (using Star-CCM+ and HEEDS) by uncertainties in the nature of the transition from laminar to turbulent flow on axissymetrical body as it invested by constant flow at zero grades incidence.
A field function has been developed to take account of physics conditions associated to boundary layer transition.
The body was located on air first and on ground later. Taking account of ground effect there are considerated two difference approach: with or without wheels. The two methods lead to similar results.
The calculation results still have to be validated experimentally. Especially it has to be investigated how surface irregularities of real cycle affect the transition location.

Bibliography

[1] Th. Lutz and S. Wagner*Numerical Shape Optimization of Natural Laminar Flow Bodies*

[2] http://www.policumbent.it

[3] https://www.popularmechanics.com

[4] http://www.aerovelo.com

[5] Th. Lutz and S. Wagner*Drag Reduction and Shape Optimization of Airship Bodies*

[6] Parsons, Jerome S. Goodson, Raymond, *The Optimum Shaping of Axisymmetric Bodies for Minimum Drag in Incompressible Flow.*

[7] André Bakker, *Applied Computational Fluid Dynamics*

[8] CD-Adapco, STAR-CCM+ Guide

[9] David A. Dress, *Drag Mesurement on a Laminar-Flow Body of Revolution in the 13.Inch Magnetic Suspension and Balanced System*, from NASA Technical Paper 2895.

[10] R. Wuilbercq, F. Pescetelliy, E. Minisciz, R. E Brownx, *Influence of Boundary Layer Transition on the Trajectory Optimisation of a Reusable Launch Vehicle*

[11] Daniel Nelson, Laminar vs Turbulent Flow, *https://sciencetrends.com/the-difference-between-laminar-and-turbulent-flow/*